Carbon dynamics at the river-estuarine transition: a comparison among tributaries of Chesapeake Bay.

Paul A. Bukaveckas
Center for Environmental Studies
Virginia Commonwealth University
Richmond, Virginia, USA

Submitted to: Biogeosciences
August 3, 2021
revised December 17, 2021
second revision June 10, 2022

Corresponding author: Paul Bukaveckas (pabukaveckas@vcu.edu)

Keywords: carbon, estuaries, mass balance CO_2 flux

Abstract

Sources and transformation of carbon (C) were quantified using mass balance and ecosystem metabolism data for the upper segments of the James, Pamunkey and Mattaponi Estuaries. The goal was to assess the role of external (river inputs & tidal exchange) vs. internal (metabolism) drivers in influencing the forms and fluxes of C. C forms and their response to river discharge differed among the estuaries based on their physiographic setting. The James, which receives the bulk of inputs from upland areas (Piedmont and Mountain), exhibited a higher ratio of inorganic to organic C, and larger inputs of particulate organic C (POC). The Pamunkey and Mattaponi receive a greater proportion of inputs from lowland (Coastal Plain) areas, which were characterized by low dissolved inorganic C (DIC) and POC, and elevated dissolved organic C (DOC). I anticipated that transport processes would dominate during colder months when discharge is elevated and metabolism is low, and that biological processes would predominate in summer, leading to attenuation of C through-puts via de-gassing of CO_2. Contrary to expectations, highest retention of organic C occurred during periods of high through-put, as elevated discharge resulted in greater loading and retention of POC. In summer, internal cycling of C via production and respiration was large in comparison to external forcing despite the large riverine influence in these upper estuarine segments. The estuaries were found to be net heterotrophic based on retention of organic C, export of DIC, low primary production relative to respiration, and a net flux of CO_2 to the atmosphere. In the James, greater contributions from phytoplankton production resulted in a closer balance between production and respiration, with autochthonous production exceeding allochthonous inputs. Combining the mass balance and metabolism data with bioenergetics provided a basis for estimating the proportion of C inputs utilized by the dominant metazoan. The findings suggest that invasive catfish utilize 15% of total organic C inputs and up to 40% of allochthonous inputs to the James.

Non-technical summary: Inland waters play an important role in the global carbon cycle by storing, transforming and transporting carbon from land to sea. Comparatively little is known about carbon dynamics at the river-estuarine transition. A study of tributaries of Chesapeake Bay showed that biological processes exerted a strong effect on carbon transformations. Peak carbon retention occurred during periods of elevated river discharge and was associated with trapping of particulate matter.

1. Introduction

Inland waters occupy a small proportion of surface area but play a disproportionately large role in landscape-scale C fluxes (Cole et al. 2007; Butman et al. 2016; Tranvik et al. 2018; Holgerson and Raymond 2016). River networks act as transport systems delivering C products of mineral weathering (DIC) and plant decomposition (DOC, POC) from the terrestrial realm to the coastal ocean (Meybeck 2003). Inland waters also function as reactors in which biotic and abiotic processes act to augment, transform or attenuate C fluxes. Aquatic primary production supplements terrestrial DOC and POC inputs, and by providing more labile forms of C, may facilitate the decomposition of older, recalcitrant terrestrial C. Decomposition of aquatic and terrestrial organic matter returns C to the atmosphere, which, along with C sequestration via sediment burial, results in the attenuation of C fluxes to the coastal zone (Richey et al. 2002; Vorosmarty et al. 2003; Middelburg and Herman 2007; Tranvik et al. 2009). Acting against these processes are fluvial forces that hasten through-puts of C and favor transport over processing. Along the flowpath from mountains to the sea, aquatic systems differ greatly in their capacity to attenuate C fluxes depending on factors such as water residence time, ecosystem metabolism and capacity for sediment accrual. Relatively complete C budgets are relatively rare, in part due to the effort involved in quantifying C fluxes from various sources (Hanson et al. 2015).

Estuaries are potentially important sites for C processing and transport given that they intercept the bulk of terrestrial runoff to the oceans. They contain complex mixtures of organic matter originating from diverse sources including terrestrial inputs, estuarine primary production, lateral inputs (e.g., tidal marshes and floodplain forests), and marine-derived organic matter (Raymond and Hopkinson 2003; Tzortziou et al. 2008). As a result, estuarine organic matter includes a complex mixture of compounds that differ in chemical composition and bioavailability. Most of the organic matter delivered by rivers to estuaries is of terrestrial origin, though recent work suggests that autochthonous riverine sources may be important during periods of low river flow (Hosen et al. 2021). The quantity and quality of riverine organic matter is dependent in part on forms of terrestrial vegetation and the extent to which this material is altered by photochemical and microbial processes along the flowpath from upland areas through river networks (Raymond and Bauer 2000; Stedmon et al. 2006; Creed et al. 2015; Zametske et al. 2018; Voss et al. 2020).

Historically, terrestrial organic matter inputs were considered largely recalcitrant in part due to their age and their high C:N ratio, though bioassay experiments and non-conservative mixing curves indicate that a fraction is labile (e.g., Moran et al. 1999; Wiegner and Seitzinger 2001). del Giorgio and Pace (2008) showed that the Hudson River Estuary acted as a pipe transporting terrestrial DOC seaward while also functioning as a reactor whereby bacterial activity decomposed POC generated via autochthonous production. Raymond and Hopkinson (2003) showed that estuarine primary production contributes significant quantities of "young" DOC which fueled the majority of heterotrophic respiration. In the context of assessing estuarine influences on C transport and retention, comparatively little attention has been focused on processes occurring at the river-estuarine transition.

Tidal freshwaters occur at the transition from riverine to estuarine conditions. They are a common feature of river-dominated estuaries throughout the world, but have received relatively little attention for their role in modifying elemental fluxes from land to sea (Hoitink and Jay 2016; Ward et al. 2017; Jones et al. 2020). A key feature of tidal freshwaters is the occurrence of bi-directional flows associated with incoming and outgoing tides (Jones et al. 2017). The combination of freshwater and tidal conditions arises because tidal forces propagate inland beyond the point where mixing of fresh and marine waters occurs. The back and forth of tidal flows reduces net seaward movement resulting in longer transit time that allows for the development of plankton communities and the potential for greater biological influence on C forms and retention. Our prior work in the James Estuary has documented higher rates of ecosystem metabolism in the tidal freshwater segment relative to adjacent riverine and lower estuarine segments (Tassone and Bukaveckas 2019; Bukaveckas et al. 2020). High rates of metabolism and depletion of dissolved inorganic nutrients was associated with the presence of chlorophyll-a and productivity maxima in the tidal fresh zone (Bukaveckas et al. 2011; Qin and Shen 2017). Other studies have also documented tidal freshwaters as biogeochemical hotspots (Vincent et al. 1996; Muylaert et al. 2005; Hoffman et al. 2008; Lionard et al. 2008; Amann et al. 2015; Young et al. 2021; Xu et al. 2021).

Long water residence time and high rates of ecosystem metabolism in the tidal fresh zone may favor the importance of internal processes (production and respiration) over external (hydrologic) forces in regulating C throughputs. During periods of low river discharge, longer

105 water residence in the estuary allows accrual of phytoplankton biomass and greater
106 phytoplankton production, which may result in net autotrophy and greater export of organic C
107 relative to DIC. Alternatively, the production of autochthonous labile C may facilitate
108 mineralization of allochthonous C inputs ("priming effect") resulting in CO_2 release and
109 attenuation of organic and total C exports (Bianchi 2011; Steen et al. 2015; Ward et al. 2016).
110 During periods of elevated discharge, freshwater replacement time in the upper estuary is short,
111 thereby favoring transport over retention. However, our recent work has shown that the bulk of
112 N and P retention in the tidal fresh zone of the James Estuary occurs during periods of high
113 sediment loading (Bukaveckas et al. 2018). Although retention of dissolved N and P was highest
114 during peak production in summer, the trapping of particulate N and P in winter accounted for
115 the bulk of total N and P retention. These findings suggest that retention of particulate and total
116 C may be highest during periods of elevated river discharge.

117 The goal of this study was to assess the relative importance of external (river inputs & tidal
118 exchange) vs. internal (metabolism) drivers in influencing C forms and retention in the upper
119 estuary. Mass balance results and ecosystem metabolism data were used to assess C inputs,
120 outputs, transformation and retention in the tidal fresh segments of the James, Pamunkey and
121 Mattaponi estuaries. A key difference among the estuaries is their geographic setting across
122 lowland (Coastal Plain) and upland (Piedmont and Mountain) areas (Figure 1). Freshwater
123 inputs to the James tidal fresh segment are largely (90%) derived from upland sources (i.e.,
124 above the Fall Line), whereas local (Coastal Plain) tributaries contribute ~10% (based on the
125 proportion of contributing area below the Fall Line). By contrast the Pamunkey and Mattaponi
126 Estuaries receive a greater proportion of freshwater inputs from local (Coastal Plain) sources
127 (36% and 51%, respectively). Higher sediment yield from upland sources should result in
128 greater POC inputs to the James relative to the Pamunkey and the Mattaponi. I also expected
129 that higher GPP and R in the phytoplankton-dominated James Estuary would exert a stronger
130 influence on C transformations relative to the Pamunkey and Mattaponi, which are dominated by
131 submerged and emergent aquatic vegetation. Lastly, extensive floodplain and wetland areas
132 along the Pamunkey and Mattaponi would be expected to contribute greater DOC inputs relative
133 to the James. For the James Estuary, C mass balance and metabolism data were used to estimate
134 allochthonous and autochthonous inputs and to assess constraints on food web energetics.

2. Methods

2.1 Study Sites. This study focuses on the upper segments of the two southern tributaries of Chesapeake Bay (James and York Estuaries), the latter of which is comprised of two sub-estuaries (Pamunkey and Mattaponi). This is the third in a series of papers that rely in part on comparisons among these estuaries to draw inferences about processes occurring at the river-estuarine transition. Previous papers focused on the influence of storm events on river and estuarine metabolism and water quality (Bukaveckas et al. 2020), and on factors regulating water clarity and primary production (Henderson & Bukaveckas 2021). The proximity of the estuaries facilitated frequent sampling (1-2 week intervals) that is needed to characterize C fluxes. The study reach within the James Estuary is the tidal fresh segment, which extends 88 km from the Fall Line (Richmond, VA) to the confluence with the Chickahominy River, and accounts for ~50% of the length of the estuary. Study reaches for the Pamunkey and Mattaponi Estuaries encompassed the tidal fresh and oligohaline segments, extending 86 km to their confluence with the York Estuary. The river basins fall within the Temperate Deciduous Forest biome. Though highly fragmented, the area is still predominantly rural and forested (>70%) with small contributions from agricultural lands (row crops and hay fields; 23%) and urban-suburban areas (6%; Smock et al. 2005). The predominant trees include a variety of oaks, hickories, sweetgum, tuliptree and loblolly pine. Floodplain forests along the Pamunkey and Mattaponi are dominated by bald cypress, swamp black gum and water tupelo. Soils of the region are old and highly weathered, with ultisols predominating over much of the area.

2.2 Data Collection. For the James, I am able to present a relatively complete C budget inclusive of Fall Line loads, local tributary inputs and tidal fluxes of inorganic and organic fractions (DIC, DOC, POC). These results are based on data collected from river and estuarine stations over a 10-year span (2010-2019). For the Pamunkey and Mattaponi, the scope is more limited both in the time span over which data were collected (2017-2019) and, due to the lack of data on Fall Line DIC and chloride inputs, which precludes estimation of tidal exchange using Cl mass balance. For the James and Pamunkey, previously published estimates of GPP and ER derived from in situ diel oxygen cycles are used to assess their effect on C transformations. Seasonal patterns in CO_2 concentrations and air-water exchange are provided for all three estuaries.

2.3 C Inputs & Estuarine Export. External C loads for the three estuaries were derived from (a) measured discharge and concentration at the Fall Line, and (b) estimated contributions from ungauged tributaries below the Fall Line. Fall Line loads were based on data collected by the USGS at gauging stations located on the James, Pamunkey and Mattaponi Rivers. Fall Line samples were collected at approximately monthly intervals, with supplemental samples collected during periods of high discharge. Approximately 200 measurements of DOC and POC were obtained at each of the gauging sites over the 10-year span (Table 1), along with continuous measurements of river discharge. For the James, the USGS data were supplemented by measuring DIC and Cl at the Fall Line at 1-2 week intervals during 2012-2019 (189 samples collected). Seasonal, inter-annual and discharge-dependent variation in riverine C concentrations was analyzed using Generalized Additive Models (see Statistics). The models were used to predict daily concentrations at each site, and, in combination with daily discharge, to derive daily loading values at the Fall Line. Local (ungauged) runoff was estimated as a constant fraction of the daily Fall Line discharge based on the proportion of catchment area represented by tributaries entering below the Fall Line. Daily concentrations were used in combination with Fall Line discharge, below Fall Line discharge, and total discharge to derive daily input and export fluxes. Daily fluxes were summed over the budget interval (typically 1-2 weeks) and used, in conjunction with the change in mass of Cl in the estuary between the start and end of each interval, to solve for the net tidal flux of Cl.

$$\textit{Estuary Cl Mass}_{t+1} = \textit{Estuary Cl Mass}_{t} + \textit{Riverine Cl} - \textit{Export Cl} \pm \textit{Net Tidal Cl} \quad (1)$$

The mass of Cl required to balance each budget interval was used in combination with measurements of Cl concentrations in tidal inflow and outflow, as represented by stations located on either side of the seaward boundary of our study reach (JMS69 and JMS56), to derive the effective volume of tidal exchange. This represents the volume of "new" water entering the study reach from the lower estuary with each tidal cycle. The James has an elongate shape that is typical of estuaries that occupy flooded river valleys. The back and forth of tidal flows means that the bulk of the water leaving on an outgoing tide returns on the subsequent incoming tide, and only a small proportion of the large tidal flux is "new" water. For the James, the effective volume of exchange is equivalent to 8% of the tidal prism (Bukaveckas and Isenberg 2013). For this study, estimates of the volume of tidal exchange were derived for each budget interval (N =

309 for 2011-19). The effective volume of exchange was used along with measured C concentrations of tidal inflows and outflows to determine the net exchange of C at the seaward boundary of the study reach. Net tidal fluxes for each budget interval were aggregated to monthly values and presented as daily areal values for comparison to riverine input and export fluxes. Lastly, monthly estimates of estuarine C retention were derived based on the difference between input and output fluxes taking into account changes in mass storage within the estuary.

$$Estuary\ C\ Mass_{t+1} = Estuary\ C\ Mass_t + Riverine\ C - Export\ C \pm Net\ Tidal\ C \pm Retention \quad (2)$$

For DIC, our estimation of retention also took into account air-water CO_2 exchange (see below).

2.5 Estuarine Metabolism. Previously published estimates of Gross Primary Production (GPP) and Ecosystem Respiration (ER) were used to assess internal C transformations for the James and Pamunkey (Bukaveckas et al. 2020). Rates of metabolism were derived from continuous (15 min) monitoring of dissolved oxygen at stations located within our study segments of the James and Pamunkey (Figure 1). The James monitoring station is located at the VCU Rice Center Research Pier, approximately 2 km from our JMS75 sampling location. The Pamunkey station (White House Landing) is operated by the Virginia Institute of Marine Science and located near the mid-point of our study segment. Similar equipment (YSI 6600 or EXO sondes) and protocols are used at the two stations including routine (2-3 week) maintenance and calibration of sondes as per manufacturer recommendations. Daily GPP and ER were derived using the single-station open-water method. Following Caffrey (2003; 2004), 15-minute DO measurements were smoothed to 30-minute averages and multiplied by water depth to obtain areal rates of oxygen flux at 30 minute intervals throughout the day.

$$O_2\ flux\ (g\ O_2\ m^{-2}\ d^{-1}) = (DO_{t2}\text{-}DO_{t1}) * Water\ Depth - AE \quad (3)$$

Atmospheric exchange (AE) was derived at 30-minute intervals based on water column DO saturation and a generic estuarine gas transfer coefficient. A previous analysis using 23 years of station data for the James showed that estimates of atmospheric exchange derived from oxygen saturation and the fixed gas transfer coefficient were not significantly different from exchange coefficients derived using variable water velocity and wind speed (Tassone and Bukaveckas 2019). ER was derived by extrapolating nightly O_2 fluxes to a 24-hour period. GPP was derived

as the sum of daytime oxygen production and ER during daylight hours. Oxygen-based values were converted to C assuming a photosynthetic quotient of 1.2 and a respitory quotient of 1.

2.6 Sampling and Analysis. Methods were described previously (Bukaveckas et al. 2011; Bukaveckas et al. 2020; Henderson and Bukaveckas 2021) and are summarized here. Data were collected from 4 stations in the James tidal fresh segment, 3 stations in each of the Pamunkey and Mattaponi study reaches, and one tributary stream (Kimages Creek) located at the VCU Rice Center (Figure 1; Table 1). Estuarine sites were sampled by boat in the main channel except in the upper, narrow sections of the Pamunkey and Mattaponi where samples were collected from shore in areas of active flow. Owing to vertically well-mixed conditions (no temperature or salinity stratification) water samples and in situ measurements were obtained near the surface (~0.5 m). Water temperature and salinity were measured using a YSI Pro DDS sonde. The partial pressure of carbon dioxide in water and air was measured in the field using a PP Systems EGM 4 portable infrared CO_2 analyzer calibrated at 0 and 2000 ppm. Water samples were analyzed for chlorophyll-a (CHLa), POC, DIC, DOC and Cl. Samples for CHLa and POC were filtered through Whatman GF/A glass filters (0.5-µm nominal pore size). Filters for CHLa analyses were extracted for 18 h in buffered acetone and analyzed on a Turner Design TD-700 Fluorometer (Arar and Collins 1997). Filters for POC analysis were dried at 60 C for 48 h, fumed with HCl to remove inorganic carbon and analyzed on a Perkin–Elmer CHN analyzer. Chloride concentrations were determined using a Skalar segmented flow analyzer by the ferriccyanide method (APHA 1998). Samples for DIC and DOC were filtered in the field through Whatman GF/A filters and analyzed using a Shimadzu TOC analyzer.

2.7 Air-Water CO_2 Fluxes. Air-water exchange of CO_2 was calculated using the equation from Cai and Wang (1998):

$$\text{Flux } CO_2 = K_T K_H (pCO_{2\text{-water}} - pCO_{2\text{-air}}) \quad (4)$$

where K_T is the gas transfer velocity, K_H is the solubility constant and pCO_2 is the partial pressure of CO_2 in water and air. The solubility constant was derived according to the equation of Weiss (1974) taking into account water temperature and salinity recorded at the time of CO_2 measurement. Gas transfer velocities were initially derived from daily average wind speed (U10 corrected) measured at the VCU Rice Center Research Pier (James) and the Taskinas Creek NERR station (Pamunkey and Mattaponi). Gas transfer velocities derived from wind speed

252 generally fell within the range of 1 to 1.5 m d^{-1}, which is low in comparison to the global average
253 (5.7 m d^{-1}, Raymond et al. 2017) and to values that are considered appropriate for large rivers
254 (4.3 m d^{-1}, Alin et al. 2011; Reiman and Xu 2019). Based on these considerations, a value of 4.3
255 m d^{-1} was used for all calculations (see Discussion for further consideration of gas transfer
256 velocities).

257 2.8 Statistics. Generalized Additive Models (GAMs) were used to model river and estuarine C
258 and Cl concentrations based on discharge, day of year (to capture seasonal patterns) and decimal
259 date (to depict inter-annual variation). GAMs are gaining increasing usage for modeling water
260 chemistry due to their ability to account for non-linear effects and to fit trends of a form that is
261 not known *a priori* (Morton & Henderson 2008; Murphy et al. 2019; Yang and Moyer 2020;
262 Wiik et al. 2021). The GAM analysis was performed using the "mgcv" package in R (Wood
263 2006). The package default thin plate regression spline was used to depict the effect sizes of
264 discharge and decimal date; a cyclic cubic regression spline was used to depict seasonal effects.
265 The default output for the effect size was shifted to center on the mean of the modeled dependent
266 variable to show the response of the GAM model within the range of dependent variable values.

267

268 # 3. Results

269 3.1 Estuarine Hydrology

270 The James, Pamunkey and Mattaponi Rivers exhibit similar hydrographs with highest monthly
271 average discharge during January-May and lowest discharge in July-November (Figure 2).
272 Average monthly discharge in winter-spring is approximately 4-fold higher in comparison to
273 summer-fall. Median freshwater replacement times (FRT), taking into account Fall Line inputs
274 plus local (ungauged) tributaries, were 30 d (James), 46 d (Mattaponi) and 60 d (Pamunkey)
275 during the period of study. The mass of Cl in the James tidal fresh segment varied by >20-fold
276 from seasonal minimum values during high discharge (~7 mg L^{-1}) to peak values (>100 mg L^{-1})
277 during summer base flow (Figure 3). These seasonal increases in estuarine Cl were most
278 pronounced in summers with low freshwater inputs (e.g., 2012, 2017, 2019). Despite the large
279 seasonal variation, Cl changed relatively slowly within the estuary (median = 0.5 % d^{-1}) as input
280 and output fluxes largely offset. In late summer (August-October), the development of strong Cl

gradients across the seaward boundary of the study reach resulted in high rates of Cl gain and loss via tidal exchange. As the lower tidal fresh segment accounts for the bulk of total volume (80%), increases in Cl at the seaward end of the study reach had a large effect on estuarine Cl mass. By volume, the effective tidal exchange derived from the Cl mass balance was equivalent to 7.4% (median) and 14 ± 1% (mean and SE) of the tidal prism.

3.2 Discharge Effects on River and Estuarine C

Discharge was a significant factor influencing riverine C concentrations, though the strength of these effects differed among C fractions and among the three tributaries. Increasing discharge was associated with increasing river DOC in the Mattaponi (from 6 to 12 mg L^{-1}) and Pamunkey (from 5 to 9 mg L^{-1}), but had little effect on James River DOC, which was generally low over the range of observed discharge (3-4 mg L^{-1}; Figure 4). Generalized Additive Models incorporating discharge, seasonal and inter-annual variation accounted for 50 to 81% of the variation in river DOC (Table 2). Increasing discharge was associated with large increases of POC in the James River (up to 20 mg L^{-1}). The effects of discharge on river POC were weaker in the Mattaponi and Pamunkey, where concentrations were generally low over the range of discharge (<2 and <4 mg L^{-1}, respectively). Increasing discharge was associated with large decreases in DIC of the James River (from 20 to 1 mg L^{-1}). Overall, increasing discharge resulted in higher DOC concentrations in the Pamunkey and Mattaponi Rivers, higher POC concentrations in the James River, and lower DIC concentrations in the James River.

Although increases in discharge had a positive effect on riverine DOC and POC, estuarine concentrations were only weakly, and in some cases negatively affected by increasing discharge (Figure 5). In the James, estuarine DOC concentrations were typically higher than riverine values, such that increases in river discharge resulted in a reduction in estuarine DOC. In the Pamunkey and Mattaponi, increasing discharge had little effect on estuarine DOC as estuarine concentrations were similar to river concentrations. Discharge was not a significant predictor of variation in DOC for the Pamunkey and Mattaponi Estuaries (Table 2). Similar findings for POC showed weak seasonal, inter-annual and discharge dependent effects and a low proportion of explained variation for the Pamunkey and Mattaponi Estuaries. In contrast, POC concentrations in the James Estuary were strongly influenced by season, with predicted concentrations rising from 1 to 2 mg L^{-1} during winter to summer. POC concentrations were

negatively related to discharge. Increasing discharge had a significant negative effect on DIC in all three estuaries, which decreased by 5-6 mg L^{-1} over the observed range of discharge. Overall, these findings show that river discharge had strong negative effects on estuarine DIC, but little influence on estuarine DOC and POC. Significant seasonal variation in POC was observed in the James, but not the Pamunkey or Mattaponi.

3.3 Estuarine pCO_2

GAM analysis revealed significant seasonal and discharge-dependent variation in estuarine pCO_2 (Table 2). The effects of discharge on estuarine pCO_2 differed among the 3 tributaries (Figure 6). In the Pamunkey and Mattaponi, there was little effect of discharge, except in the upper quartile of the range, which was associated with rising estuarine pCO_2. In the James, estuarine pCO_2 increased linearly over the lower one-third range of discharge, and thereafter plateaued. The Mattaponi and Pamunkey exhibited large seasonal variations in estuarine pCO_2. Peak summer concentrations (~2600 ppmv) were two-fold higher in comparison to winter minimum values (~1200 ppmv;). A more complex seasonal pattern was observed in the James with bi-model peaks in spring and fall (850 and 1250 ppmv, respectively) bracketing low concentrations in mid-summer. In summer, significantly lower pCO_2 was observed at sites located at the CHLa maximum (JMS75 = 789 ppmv, JMS69 = 644 ppmv) relative to stations in the upper tidal fresh segment (JMS99 = 1007 ppmv) and the most seaward station (JMS56 = 909 ppmv; $p < 0.01$). The two stations located at the CHLa maximum were the only sites to exhibit periodic under-saturation of pCO_2 (Supplemental Figure 4). The low values at these stations were not observed in winter. There was little longitudinal variation in pCO_2 among stations in the Pamunkey and Mattaponi. Overall, annual average concentrations in the Pamunkey (2010 ± 117 ppmv) and Mattaponi (1900 ± 120 ppmv) were more than 2-fold higher relative to the James (784 ±77 ppmv). Higher pCO_2 concentrations in the Pamunkey and Mattaponi estuaries were associated with larger air-water CO_2 fluxes (2.97 ± 0.17 and 2.77 ± 0.17 g C m^{-2} d^{-1}, respectively) relative to the James (0.87 ± 0.05 g m^{-2} d^{-1}; Figure 7). Strong seasonal patterns were observed in the Pamunkey and Mattaponi with monthly average fluxes ranging from 1-2 g m^{-2} d^{-1} in winter to 3-4 g m^{-2} d^{-1} in summer, whereas fluxes from the James were similar year-round (~1 g m^{-2} d^{-1}).

3.4 C Fluxes & Retention

C fluxes into and out of the James Estuary varied seasonally (Figure 8). DOC inputs followed expected seasonal patterns with peak values during months with elevated discharge (January-May) and minimum values during predominantly low discharge in July-November. Seasonal variation in DOC inputs was closely matched by export fluxes. Net tidal fluxes were negligible by comparison owing to small differences in concentration across the segment boundary. Monthly DOC retention was generally negative, indicating net export of DOC. On an annual basis, the DOC balance was -0.10 ± 0.02 g m^{-2} d^{-1}, with export exceeding inputs by 11 ± 5%. Riverine inputs of POC varied seasonally with highest values in January-May and generally low values in June-December. By contrast, estuarine export of POC was consistently low throughout the year. As a result, POC retention was highest in January-May. Net tidal fluxes were positive indicating a loss of POC with each tidal cycle, but these fluxes were small in comparison to river inputs. On an annual basis, the net retention of POC was 0.59 ± 0.11 g m^{-2} d^{-1}, corresponding to 72 ± 4% of inputs. DIC input and output fluxes followed a similar pattern as for DOC, with peak values in months with high discharge. Taking into account estuarine export and atmospheric fluxes, the James was a net source of DIC with losses (4.25 g m^{-2} d^{-1}) exceeding inputs (2.82 g m^{-2} d^{-1}) by 51%.

Our mass balance analysis does not explicitly consider the role of point source inputs in the estuarine C budget. Point sources that discharge to the tidal fresh segment of the James are principally wastewater treatment plants, and some industries associated with the Richmond metro area. The volume of effluent discharged to the James is small (annual average = 15-21 m^3 s^{-1} during 2007-14) in comparison to annual average river discharge (~225 m^3 s^{-1}). But as effluent may contain elevated C concentrations, point sources could potentially contribute an appreciable fraction of C inputs. Point sources typically do not report C concentrations as part of their effluent monitoring, therefore we carried out a 2-year study of DIC, DOC and POC concentrations in effluent from the largest point source (City of Richmond WWTP). Effluent POC concentrations (1.54 ± 0.13 mg L^{-1}) were comparable to riverine values, whereas effluent DOC (13.1 ± 1.2 mg L^{-1}) and DIC (22.7 ± 1.6 mg L^{-1}) were two-fold higher relative to riverine concentrations. These values were extrapolated to all point source inputs to the James as a first approximation of their potential importance to the estuarine C budget. Daily average POC loads from point sources were too small to appreciably affect our estimate of estuarine POC retention. Point source inputs of DOC (0.21 g m^{-2} d^{-1}) and DIC (0.36 g m^{-2} d^{-1}) were equivalent to 23% and

12% (respectively) of riverine inputs. Taking into account point source contributions, the mass balance shows that the James tidal fresh segment is a net sink for DOC (0.12 g m^{-2} d^{-1}) and POC (0.61 g m^{-2} d^{-1}) and a net source of DIC (1.07 g m^{-2} d^{-1}). Overall, the James tidal fresh segment was nearly in balance (within 6%) for total C inputs and outputs.

Annual average DOC loads to the Pamunkey (0.67 ± 0.11 g m^{-2} d^{-1}) and Mattaponi (0.89 ± 0.12 g m^{-2} d^{-1}) were similar to the James (0.91 ± 0.12 g m^{-2} d^{-1}) on an areal basis. Seasonal variation in DOC inputs followed patterns in discharge with peak values in winter-spring and minimum values in summer-fall (Figure 9). Export fluxes closely matched river inputs on a seasonal basis, and balanced to within 10% on an annual basis. Riverine POC inputs to the Pamunkey and Mattaponi were considerably lower relative to the James. For the James, POC inputs were nearly equal to DOC inputs, whereas for the Pamunkey and Mattaponi, DOC accounted for the bulk of OC inputs (79% and 86%, respectively). Export of POC from the Pamunkey and Mattaponi matched inputs to within 10% on an annual basis.

3.5 Estuarine Metabolism

Rates of GPP and ER were compared to standing stocks (areal values) of DIC and POC to assess the potential influence of C fixation and remineralization on estuarine C concentrations (Figure 10). In the James, GPP and ER followed expected seasonal patterns with peak values (3.5 – 4.0 g C m^{-2} d^{-1}) during June-September and low values (<1 g C m^{-2} d^{-1}) in colder months. GPP and ER tracked closely throughout the year, with ER exceeding GPP in colder months, and being equal, or occasionally smaller (June-July) than GPP in warmer months. C fluxes associated with GPP and ER were small in comparison to ambient concentrations of DIC, which ranged from 30 to 40 g m^{-2}. By contrast, POC production via GPP was comparable to ambient concentrations of POC, which ranged from 3 g m^{-2} in colder months to 6 g m^{-2} in warmer months. Metabolism of the Pamunkey Estuary was lower and more heterotrophic in comparison to the James. ER varied seasonally from 0.5 to 1.8 g C m^{-2} d^{-1}, whereas GPP was persistently low throughout the year (< 0.5 g C m^{-2} d^{-1}). Standing stocks of DIC were large by comparison, ranging from 10 to 40 g m^{-2}. GPP was small in comparison to standing stocks of POC (3 to 5 g m^{-2}).

4.0 Discussion

4.1 Riverine C Inputs & Estuarine Concentrations

An analysis of C dynamics in the upper portions of the James, Mattaponi and Pamunkey estuaries revealed differences in dominant forms of C and variable responses to changes in river discharge. The James was dominated by products of mineral weathering as DIC accounted for 73% of total C with smaller contributions from DOC (20%) and POC (7%). By contrast, organic forms accounted for a larger fraction (49%) of total C in the Pamunkey and Mattaponi. These differences are attributed to variable contributions from local (Coastal Plain) vs. upland (Mountain and Piedmont) runoff. The James Estuary receives inputs from a large catchment with the bulk of runoff (90%) derived from above the Fall Line. By contrast, the Pamunkey and Mattaponi Estuaries receive a greater proportion of their inputs from local tributaries situated within the Coastal Plain. Local floodplains and tidal marshes contribute DOC, while the predominantly sandy soils of the Coastal Plain have low capacity for retaining DOC, and contribute little DIC. Differences in source waters may also account for contrasting response in river and estuarine C to high discharge events. Larger increases in POC were observed during discharge events in the James, relative to the Pamunkey and Mattaponi. Prior studies documented higher sediment yields from Mountain and Piedmont regions in comparison to the Coastal Plain (Gellis et al. 2009). In the James River, changes in C concentrations with increasing discharge were asynchronous as DIC was negatively related to discharge, whereas POC showed a positive relationship. These findings suggest that DIC export from the watershed is limited by weathering rates (source limited) whereas POC export is transport limited (Wymore et al. 2021). For DIC, this resulted in a dilution response in both the river and estuary, whereas high discharge resulted in a flushing response (enrichment) of POC in the river and estuary. Dilution of estuarine DIC during high discharge was also reported in the nearby Delaware Estuary and linked to reductions in acid neutralizing capacity and greater sensitivity to acidification (Joesef et al. 2017). For DOC, a strong flushing response was observed in the Pamunkey and Mattaponi Rivers, but not the James. Higher DOC concentrations following storm events has been attributed to greater leaching from soils due to higher water elevation and soil inundation (Zarnetske et al. 2018; Patrick et al. 2020). The extensive wetlands and floodplains along the Mattaponi and Pamunkey likely serve as source areas for DOC. Prior work showed that differences in source waters played a role in determining underwater light conditions in these estuaries, as light attenuation in the James was strongly regulated by suspended particulate matter, whereas dissolved organic matter had a greater role in attenuating

light in the Pamunkey and Mattaponi estuaries (Henderson and Bukaveckas 2021). Overall, our findings showed strong concentration-discharge relationships in riverine waters, whereas estuarine responses were weaker and more variable. Inter-estuarine differences in C forms and response to discharge were linked to differences in the physiographic setting of the estuarine catchments.

4.2 C Mass Balance

The tidal freshwater segment of the James Estuary was a net sink for POC and DOC, and a net source of DIC. On an annual basis, external organic matter inputs were attenuated by 28% (±3) within the tidal fresh segment. The mass balance indicates that a high proportion (72%) of POC inputs were retained in the tidal fresh segment and that retention of POC accounted for the bulk (84%) of organic matter retention. Amann et al. (2012) similarly documented high retention of POC in tidal freshwaters of the River Elbe. The transition from fluvial to tidal conditions favors the settling of suspended particulate matter, which contained ~10-20% organic matter (Bukaveckas et al. 2019). Peak retention occurred during periods of elevated discharge when inputs of particulate matter to the estuary were highest. Our findings do not support the view that inlands waters function primary as transport systems ("pipes") during periods of elevated discharge (Zarnetske et al. 2018) as the bulk of organic matter retention occurred during high flows in winter, and was associated with the retention of particulates. High retention of particulate C is consistent with prior results showing that peak retention of N and P occurred during colder months with elevated river discharge (Bukaveckas and Isenberg 2013). Retention of dissolved N and P was highest during low discharge in summer, but this accounted for a relatively small proportion of total N and P retention on an annual basis. For C, as for N and P, the mass of particulate matter delivered to the estuary during high discharge appears to be the most important determinant of the amount retained within the estuary. The counter-intuitive finding that peak retention occurs during periods of high transport (when "pipe" conditions might prevail) is based on a consideration of the fate of both dissolved and particulate organic matter, as the former largely passes through, while the latter is highly retained. The retention of particulate matter reflects the underlying hydrodynamics of estuaries, and lakes, where the rapid dissipation of fluvial forces promotes high retention of particulate matter during periods of elevated discharge.

For the James, atmospheric losses were a small component of the C budget, equivalent to 18% of riverine total C inputs and 15% of total C export. Volta et al. (2016) similarly report that CO_2 loss via evasion was ~15% of C export from North Sea estuaries. By contrast, CO_2 evasion from the Pamunkey and Mattaponi was appreciably greater (by 3-fold) relative to the James. Our pCO_2 concentrations for the Pamunkey were similar to those previously reported by Raymond et al. (2000), whereas our air-water flux values were higher (~3 g C m^{-2} d^{-1} vs. ~0.7 g C m^{-2} d^{-1}). Comparisons of CO_2 fluxes are complicated by uncertainty regarding atmospheric exchange (Raymond and Cole 2001; Borges et al. 2004; Raymond et al. 2017; Ward et al. 2017). Raymond et al. (2000) used what they considered a conservative exchange coefficient (1.1 m d^{-1}). More recent studies have adopted higher exchange coefficients, particularly for systems where tidal and fluvial forces likely play a greater role in determining boundary layer conditions than are predicted from wind-based models. Wind speeds are low in the upper segments of these estuaries because the prevailing winds (SSW) are nearly perpendicular to the long axis of the channel, which runs mostly east-west. Turbulence generated by strong tidal forces in shallow channels likely plays a greater role in influencing boundary conditions for gas exchange (Raymond and Cole 2001; Borges et al. 2004). These conditions support the use of higher exchange coefficients than would be derived from wind speed alone.

Tidal fluxes were not a large component of the mass balance for any of the C fractions. Although the volume of water exchanged during a tidal cycle was large (tidal prism = 28% of estuarine volume), the elongate shape of the estuary dictates that water leaving on an out-going tide returns on the subsequent in-coming tide. Results from the Cl mass balance suggest that the net tidal exchange was ~7% of the tidal prism, equivalent to 2% of estuarine volume. In addition, weak C gradients across the lower boundary of the study reach indicate that tidal inputs and outputs largely offset.

4.3 Metabolism & Carbon

Mass balance and metabolism data provide independent evidence that these estuaries are net heterotrophic. The mass balance indicates that on an annual basis the James Estuary is a sink for organic C and a source of inorganic C. This finding is consistent with the metabolism results showing that ecosystem respiration exceeds GPP. Greater heterotrophy was observed in the Pamunkey where respiration rates were comparable to the James, but GPP was substantially

lower. This finding was consistent with the observed higher CO_2 concentrations and efflux. The evasion of CO_2 from the Pamunkey and Mattaponi was large (3x) in comparison to riverine inputs of DOC and POC, whereas CO_2 loss from the James was ~50% of riverine OM inputs. Greater heterotrophy of the former is attributed to differences in hydrogeomorphology and forms of primary production. Higher chlorophyll-a values in the James indicate greater phytoplankton contributions to GPP, which brings the tidal fresh segment more closely in balance with respect to production and respiration. The Pamunkey and Mattaponi have low chlorophyll-a by comparison (Bukaveckas et al. 2020) but extensive lateral floodplains and emergent marshes (Hupp et al. 2009; Noe and Hupp 2009; Lake et al. 2013). Decomposition of terrestrial organic matter during floodplain inundation may account for the high CO_2 concentrations and air-water fluxes during high discharge conditions. Van Dam et al. (2018) similarly reported that high CO_2 losses during flooding events accounted for 30-40% of annual emissions from North Carolina estuaries. An accounting of changes in floodplain C stores before and after inundation events is needed to better understand their role in supporting respiration in these systems. Organic matter inputs following senescence of emergent vegetation may also contribute to higher rates of respiration and CO_2 evasion. Emergent plant production would not be captured in the diel dissolved-O_2 based estimates of ecosystem GPP, which may over-estimate heterotrophy in this system. Overall, C mass balance and ecosystem metabolism data show that the upper segments of these estuaries are net heterotrophic. This finding is consistent with a meta-analysis of metabolism data showing that estuaries are generally net heterotrophic (Hoellein et al. 2013), but contrasts with recent work by Brodeur et al. (2019) showing that the Susquehanna River and mainstem Chesapeake Bay are a net sink for DIC, and therefore net autotrophic. In the case of Chesapeake Bay, it may be that much of the terrestrial organic matter (or at least, the POC fraction) is captured in the tributaries, thereby favoring a prevalence of autochthony over allochthony, and GPP in excess of R.

Despite the large riverine influence in these upper estuarine segments, internal cycling of C via production and respiration was large in comparison to external forcing via fluvial and tidal exchange (Figure 11). In summer, remineralization of C via respiration was almost 2-fold greater in comparison to external DIC inputs. In winter, the balance tipped strongly in favor of external inputs as riverine DIC contributions were 3-fold greater than internal production via respiration. Internal production of POC via GPP was an order of magnitude higher than external

522 inputs of POC in summer. In winter, GPP contributions were approximately equal to external
523 inputs of POC. Based on GPP, the estimated turnover time of the POC pool was 1.5 d in
524 summer. Taking into account that 60% of POC in the James is algal (Wood et al. 2016), the
525 estimated phytoplankton turnover time was 0.9 d. The high rates of internal biological
526 processing relative to through-puts of C places the James toward the lake-end, rather than the
527 stream-river end, on the metabolism and residence time spectrum (Hotchkiss et al. 2018). This is
528 likely a consequence of tidal conditions, which allow for longer water residence time compared
529 to non-tidal rivers. Proximal nutrient inputs (from riverine and point sources) and poor water
530 clarity (due to suspended sediments), likely also contribute to the dominance of phytoplankton
531 over aquatic plants in this system. If recent increases in water clarity continue (Henderson and
532 Bukaveckas 2021), we would expect a shift toward macrophyte dominance, lower GPP:ER, and
533 a diminished influence of internal C cycling.

534 The tidal fresh segment of the James has moderately low DIC and high GPP, which raises the
535 question whether primary production is limited by the availability of inorganic C. Our data show
536 that daily autotrophic C demand is small (~10%) relative to the available DIC pool. In summer,
537 DIC requirements to sustain GPP exceed the rate of external supply via river inputs, but
538 remineralization of C via respiration is approximately equal to GPP, indicating that internal
539 cycling is sufficiently large to preclude C limitation. However, a case could be made for
540 potential C limitation of photosynthesis due to depletion of pCO2. The diffusion of CO_2 in water
541 occurs more slowly than in air, potentially resulting in depletion during periods of high
542 autotrophic demand. In the James, low CO_2, with occasional under-saturation, was observed in
543 summer at stations corresponding to the CHLa maximum. Other studies in riverine settings have
544 shown that phytoplankton can reduce CO_2 to near or below atmospheric equilibrium (Raymond
545 et al. 1997; Crawford et al. 2017). As CO_2 is energetically favored for carbon fixation, depletion
546 of CO_2 may reduce production efficiency and alter community structure by favoring taxa capable
547 of using bicarbonates. A number of prior studies have linked primary production and pCO2
548 (Jansson et al. 2012; Low-Decarie et al. 2015; Hasler et al. 2016). Our CO_2 data were collected
549 mid-morning, closer to the diel maximum than the afternoon minimum (Crosswell et al. 2017;
550 Reiman and Xu 2019), thereby potentially under-estimating CO_2 depletion. The possibility that
551 phytoplankton-driven CO_2 depletion in the James may affect production and community

552 composition cannot be discounted, though this effect appears limited to mid-summer and stations
553 located at the CHLa maximum.

554 4.4 C Sources & Consumer Energetics

555 Lastly, I consider the utility of our C mass balance for understanding trophic energetics of the
556 James food web, particularly with respect to autochthony and allochthony. Combining mass
557 balance, ecosystem metabolism and bioenergetics is a potentially powerful approach to
558 advancing our understanding of C cycles, but there are few examples, often, as in this case, due
559 to a lack of data on consumer production (Ruegg et al. 2021). From a mass flux perspective, a
560 comparison of autochthonous (GPP = 719 ± 32 g C m^{-2} y^{-1}) and allochthonous (POC= 298 ± 56,
561 DOC = 340 ± 44 g C m^{-2} y^{-1}) inputs suggests that internal C sources are nearly equal (54 ± 4%)
562 to external inputs, despite the large riverine influence in the upper estuary. These estimates can
563 be refined to better reflect availability for consumers by discounting GPP by 40% to reflect loss
564 via autotrophic respiration (Ruegg et al. 2021) and taking into account the fraction of POC and
565 DOC that is retained (28 ± 3%). By this estimate, autochthonous production contributes 70%
566 (431 g C m^{-2} y^{-1}) and allochthonous inputs 30% (203 g C m^{-2} y^{-1}) of C available to consumers.
567 These percentages are based on annualized values though their relative importance varies
568 seasonally with the majority of GPP occurring in May to October, and the bulk of POC delivered
569 in January to May.

570 Comparisons of mass fluxes may not be indicative of C supporting secondary production if
571 consumers preferentially utilize one source over another. A number of studies have suggested
572 that autochthonous sources account for a disproportionately large fraction of C assimilation due
573 to the higher nutritional quality of algae over partially decomposed terrestrial plant matter (Brett
574 et al. 2009; Thorp and Bowes 2017). Stable isotope analysis of the James food web has shown
575 that the dominant metazoans by biomass, which are benthic omnivores (catfish, adult gizzard
576 shad), carry a predominantly terrestrial C signature, whereas zooplankton and planktivorous fish
577 (juvenile gizzard shad and threadfin shad) were dependent on autochthonous C sources (Wood et
578 al. 2016). These patterns were consistent with analysis of basal resources showing that the
579 sediments in the estuary were largely (90%) comprised of terrestrial C, whereas seston contained
580 a greater fraction of autochthonous C (60% in summer).

581 The lack of secondary production data does not allow us to align C supply from autochthonous
582 and allochthonous sources with C demands of consumers. However, the rate of biomass removal
583 for one of the dominant metazoans (catfish) can be used as a first approximation of their annual
584 production. Catfish were introduced to the James during the 1970's and 1980's and now
585 dominate the fishery (Fabrizio et al. 2018), which has led to questions about their influence on
586 food webs and ecosystem processes (Greenlee and Lim 2011; Hilling et al. 2019; Schmitt et al.
587 2019). The biomass of catfish removed from the James represents a conservative estimate of
588 their annual production in that current harvest rates have not brought about declines in the catfish
589 population, indicating that annual production exceeds the amount of biomass removed (Orth et
590 al. 2017). During 2010-2020, the commercial harvest of catfish in the tidal James averaged
591 1,000,000 lbs y^{-1} (data provided by Virginia Marine Resources Commission), which taking into
592 account the area of the fresh-brackish estuary, yields a harvest rate of 8.6 kg ha^{-1} y^{-1}. In addition
593 to the commercial harvest, piscivorous birds are an important component of biomass removal.
594 Here we focus on predation by bald eagles and osprey as there are census data during the
595 breeding season (from areal surveys) and estimates of catfish contributions to adult and nestling
596 diets (from direct observations and stable isotopes; Garman et al. 2010). Based on census data
597 and bioenergetics modeling, fish consumption by bald eagles and osprey was estimated at 0.6 kg
598 ha^{-1} d^{-1} for the James tidal fresh segment. Taking into account the contribution of catfish to the
599 diet of bald eagles and osprey (~35%) yields an estimate of catfish biomass removal of 77 kg ha^{-1}
600 y^{-1}, which is ~9-fold higher than for commercial fisheries. With further corrections for the
601 moisture content (75%; Cresson et al. 2017) and C content of fish tissues (45%; Tanner et al.
602 2000), the total catfish removal by birds and commercial fishing is 0.96 g C m^{-2} y^{-1}. Their
603 trophic position in the James (trophic level = 3.1; Orth et al. 2017) suggests a production
604 efficiency of ~1% (Ruegg et al. 2021), which yields an estimated C demand to maintain this
605 level of production/harvest of 96 g C m^{-2} y^{-1}. The C demand for this introduced species
606 corresponds to 15% of C available to consumers from allochthonous and autochthonous sources.
607 Stable isotope data indicate that catfish in the James tidal fresh obtain 9% of their C from
608 autochthonous sources and 81% from allochthonous sources (Wood et al. 2016). Applying these
609 values suggests that 2% of GPP and 41% of allochthonous inputs are required to sustain current
610 levels of catfish biomass removal from the James tidal fresh. The high rate of utilization for
611 allochthonous inputs is consistent with our prior finding that consumer-mediated recycling is an

612 important component of nutrient supply, and may account for the lack of response in primary
613 production to large reductions in point source nutrient inputs (Wood et al. 2014).

614 4.5 Summary

615 This paper provides an accounting of C fluxes at the river-estuarine transition for three tributaries
616 of Chesapeake over a span of years and discharge conditions. The findings show that the
617 relative importance of external (river inputs & tidal exchange) vs. internal (metabolism) drivers
618 differed among the three estuaries based on their physiographic setting and forms of primary
619 production. Estuarine C forms were influenced by variable contributions from upland (DIC-rich,
620 POC-rich) and lowland (DOC-rich) sources. Peak organic matter retention was associated with
621 trapping of POC during high discharge conditions. Tidal exchange was not an important
622 component of the C budget, whereas biological transformations via production and respiration
623 were large in the phytoplankton-dominated James Estuary. Contrary to expectations,
624 autochthonous sources accounted for the bulk of organic matter inputs despite the large riverine
625 influence on the upper estuary. Commercial harvest data and previously derived estimates of
626 piscivory by birds provided a basis for estimating consumer C demand, albeit for a single
627 dominant species, and at a coarse (annualized) scale. Further progress in aligning C flows to
628 food web energetics depends on the availability of production data for a greater range of
629 consumers and at shorter time intervals. Bringing together C mass balance, ecosystem
630 metabolism and consumer production data would enable a potentially powerful approach for
631 advancing our understanding of how the timing and sources of C inputs constrain trophic
632 energetics.

633

634 Acknowledgements

635 Thanks to Samantha Rogers who drafted figures for this paper, to D. Hopler, S. Tassone and W.
636 M. Lee who carried out the field and lab work, and to Donald Orth for helpful discussions
637 regarding catfish in the James. I am grateful to the USGS for providing discharge, DOC and
638 POC data for Fall Line stations and to the Virginia Institute of Marine Science for making
639 available dissolved oxygen data from the Pamunkey. This paper is dedicated to Jon Cole for his

640 contributions to our understanding of C cycling in inland waters and in appreciation for his
641 ability to turn numbers into interesting stories.

642 Data availability

643 Data can be accessed upon request to the corresponding author.

644 Competing interests

645 The author declares that there is no conflict of interest.

646

Reference List

Alin, S. R., de Fatima, F.L., Rasera, M., Salimon, C.I., Richey, J.E., Holtgrieve, G.W., Krusche, A.V. and Snidvongs, A. Physical controls on carbon dioxide transfer velocity and flux in low-gradient river systems and implications for regional carbon budgets. Journal of Geophysical Research: Biogeosciences 116: G01009, 2011

Amann, T., Weiss, A. and Hartmann, J. Carbon dynamics in the freshwater part of the Elebe estuary, Germany: Implications of improving water quality. Estuarine, Coastal and Shelf Science 107: 112-121, 2012.

Amann, T., Weiss, A. and Hartmann, J. Inorganic carbon fluxes in the inner Elbe Estuary, Germany. Estuaries and Coasts 38: 192-210, 2015.

Bianchi, T. S. The role of terrestrially derived organic carbon in the coastal ocean: a changing paradigm and the priming effect. Proceedings of the National Academy of Sciences USA 108: 19473-19481, 2011.

Borges, A. V., Delille, B., Schiettecatte, L-S., Gazeau, F., Abril, G. and Frankignoulle, M. Gas transfer velocities of CO2 in three European estuaries (Randers Fjord, Scheldt, and Thames). Limnology and Oceanography 49: 1630-1641, 2004.

Brett, M. T., Kainz, M., Taipale, S. and Seshan, H. Phytoplankton, not allochthonous carbon, sustains herbivorous zooplankton production. Proceedings of the National Academy of Sciences USA 106: 21197-21201, 2009.

Brodeur, J. R., Chen, B., Su, J., Xu, Y-Y., Hussain, N., Scaboo, K.M., Zhang, Y., Testa, J.M. and Cai, W-J. Chesapeake Bay inorganic carbon: distribution and seasonal variability. Frontiers in Marine Science 6: 99, 2019.

Bukaveckas, P. A., Barry, L.E., Beckwith, M.J., David, V. and Lederer, B. Factors determining the location of the chlorophyll maximum and the fate of algal production within the tidal freshwater James River. Estuaries and Coasts 34: 569-582, 2011.

Bukaveckas, P. A., and Isenberg, W.N. Loading, transformation and retention of nitrogen and phosphorus in the tidal freshwater James River (Virginia). Estuaries and Coasts 36: 1219-1236, 2013.

Bukaveckas, P. A., and Wood, J.D. Nitrogen retention in a restored tidal stream (Kimages Creek, VA) assessed by mass balance and tracer approaches. Journal of Environmental Quality 43: 1614-1623, 2014.

Bukaveckas, P. A., Beck, M., Devore, D. and Lee, W.M. Climate variability and its role in regulating C, N and P retention in the James River Estuary. Estuarine, Coastal and Shelf Science 205: 161-173, 2018.

Bukaveckas, P. A., Katarzyte, M., Schlegel, A., Spuriene, R., Egerton, T.A. and Vaiciute, D. Composition and settling properties of suspended particulate matter in estuaries of the Chesapeake Bay and Baltic Sea regions. Journal of Soils and Sediments 19: 2580-2593, 2019.

Bukaveckas, P. A., Tassone, S., Lee, W.M. and Franklin, R.B. The influence of storm events on metabolism and water quality of riverine and estuarine segments of the James, Mattaponi and Pamunkey Rivers. Estuaries and Coasts 43: 1585-1602, 2020.

688 Butman, D., Stackpoole, S., Stets, E.G., McDonald, C.P., Clow, D.W. and Striegl, R.G. Aquatic
689 carbon cycling in the conterminous United States and implications for terrestrial carbon
690 accounting. Proceedings of the National Academy of Sciences USA 113: 58-63, 2016.

691 Caffrey, J. M. Production, respiration and net ecosystem metabolism in U.S. estuaries.
692 Environmental Monitoring and Assessment 81: 207-219, 2003.

693 Caffrey, J. M. Factors controlling net ecosystem metabolism in U.S. estuaries. Estuaries 27: 90-
694 101, 2004.

695 Cai, W.-J., and Wang, Y. The chemistry, fluxes and sources of carbon dioxide in the estuarine
696 waters of the Satilla and Altamaha Rivers, Georgia. Limnology and Oceanography 43:
697 657-668, 1998.

698 Cole, J. J., Prairie, Y.T., Caraco, N.F., McDowell, W.H., Tranvik, L.J., Striegl, R.G., Duarte,
699 C.M., Kortelainen, P., Downing, J.A., Middelburg, J.J. and Melack, J.M. Plumbing the
700 global carbon cycle: integrating inland waters into the terrestrial carbon budget.
701 Ecosystems 10: 171-184, 2007.

702 Crawford, J. T., Butman, D., Loken, L.C., Stadler, P., Kuhn, C. and Striegl, R.G. Spatial
703 variability of CO2 concentrations and biogeochemistry in the Lower Columbia River.
704 Inland Waters 7: 417-427, 2017.

705 Creed, I. F., and others. The river as a chemostat: fresh perspectives on dissolved organic matter
706 flowing down the river continuum. Canadian Journal of Fisheries and Aquatic Sciences
707 72: 1272-1285, 2015.

708 Cresson, P., Travers-Trolet, M., Rouquette, M., Timmerman, C-A., Giraldo, C., Lefebvre, S. and
709 Ernande, B. Underestimation of chemical contamination in marine fish muscle tissue can
710 be reduced by considering variable wet:dry weight ratios. Marine Pollution Bulletin.
711 123: 279-285, 2017.

712 Crosswell, J. R., Anderson, I.C., Stanhope, J.W., Van Dam, B., Brush, M.J., Ensign, S.H.,
713 Piehler, M.F., McKee, B., Bost, M. and Paerl, H.W. Carbon budget of a shallow
714 lagoonal estuary: transformations and source-sink dynamics along the river-estuary-ocean
715 continuum. Limnology and Oceanography 62: S29-S45, 2017.

716 del Giorgio, P. A., and M. L. Pace. Relative independence of organic carbon transport and
717 processing in a large temperate river: The Hudson River as both pipe and reactor.
718 Limnology and Oceanography 53: 185-197, 2008.

719 Fabrizio, M. C., Tuckey, T.D., Latour, R.J., White, G.C. and Norris A.J. Tidal habitats support
720 large numbers of invasive blue catfish in a Chesapeake Bay sub-estuary. Estuaries and
721 Coasts 41: 827-840, 2018.

722 Garman, G., Viverette, C., Watts, B. and Macko. S. Predator-prey Interactions among Fish-
723 eating Birds and selected Fishery Resources in the Chesapeake Bay: Temporal and
724 Spatial Trends and Implications for Fishery Assessment and Management. William &
725 Mary Center for Conservation Biology Technical Report #349.
726 https://scholarworks.wm.edu/ccb_reports/349, 2010.

727 Gellis, A.C. and others. Sources, transport, and storage of sediment in the Chesapeake Bay
728 Watershed. U.S. Geological Survey Scientific Investigations Report 2008–5186, 2009.

729 Greenlee, R. S., and Lim, C.N. Searching for equilibrium: population parameters and variable
730 recruitment in introduced blue catfish populations in four Virginia tidal river systems.
731 American Fisheries Society Symposium 77: 349-367, 2011.

732 Hanson, P. C., Pace, M.L., Carpenter, S.R., Cole, J.J. and Stanley, E.H. Integrating landscape
733 carbon cycling: research needs for resolving organic carbon budgets of lakes. Ecosystems
734 18: 363-375, 2015.

735 Hasler, C. T., Butman, D., Jeffrey, J.D. and Suski, C.D. Freshwater biota and rising pCO2?
736 Ecology Letters 19: 98-108, 2016.

737 Henderson, R. and Bukaveckas, P.A. Factors governing light attenuation in upper segments of
738 the James and York Estuaries and their influence on primary producers. Estuaries &
739 Coasts https://doi.org/10.1007/s12237-021-00983-6, 2021.

740 Hilling, C. D., Bunch, A.J., Emmel, J.A., Schmitt, J.D. and Orth, D.J. Growth and mortality of
741 invasive flathead catfish in the tidal James River, Virginia. Journal of Fish and Wildlife
742 Management 10: 641-652, 2019.

743 Hoellein, T. J., Bruesewitz, D.A. and Richardson, D.C. Revisiting Odum (1956): a synthesis of
744 aquatic ecosystem metabolism. Limnology and Oceanography 58: 2089-2100, 2013.

745 Hoffman, J. C., Bronk, D.A. and Olney, J.E. Organic matter sources supporting lower food web
746 production in the tidal freshwater portion of the York River estuary. Estuaries and Coasts
747 31: 898-911, 2008.

748 Hotchkiss, E. R., Sadro, S. and Hanson, P.C. Toward a more integrative perspective on carbon
749 metabolism across lentic and lotic inland waters. Limnology and Oceanography: Letters
750 3: 57-63, 2018.

751 Hoitink, A. J. F. and Jay, D.A. Tidal river dynamics: implications for deltas. Reviews of
752 Geophysics 54: 240-272, 2016.

753 Holgerson, M. A. and Raymond, P.A. Large contribution to inland water CO_2 and CH_4
754 emissions from very small ponds. Nature Geoscience doi: 10.1038/ngeo2654, 2016.

755 Hosen, J. D., K. S. Aho, J. H. Fair, E. D. Kyzivat, S. Matt, J. Morrison, A. Stubbins, L. C.
756 Weber, B. Yoon, and P. A. Raymond. Source switching maintains dissolved organic
757 matter chemostasis across discharge levels in a large temperate river network.
758 Ecosystems 24: 227-247, 2021.

759 Hupp, C. R., Pierce, A.R. and Noe, G.B. Floodplain geomorphic processes and environmental
760 impacts of human alteration along Coastal Plain rivers, USA. Wetlands 29: 413-429,
761 2009.

762 Jansson, M., Karlsson, J. and Jonsson, A. Carbon dioxide super-saturation promotes primary
763 production in lakes. Ecology Letters 15: 527-532, 2012.

764 Joesoef, A., Kirchman, D.L., Sommerfield, C.K. and Cai, W-J. Seasonal variability of the
765 inorganic carbon system in a large coastal plain estuary. Biogeosciences 14: 4949-4963,
766 2017.

767 Jones, A. E., Hodges, B.R., McClelland, J.W., Hardison, A.K. and Moffett, K.B. Residence-
768 time-based classification of surface water systems. Water Resources Research 53: 5567-
769 5584, 2017.

770 Jones, A. E., Hardison, A.K., Hodges, B.R., McClelland, J.W. and Moffett, K.B. Defining a
771 riverine tidal freshwater zone and its spatiotemporal dynamics. Water Resources
772 Research 56: e2019WRR026619, 2020.

773 Lake, S.J., Brush, M.J., Anderson, I.C. and Kator, H.I. Internal versus external drivers of
774 periodic hypoxia in a coastal plain tributary estuary: the York River, Virginia. Marine
775 Ecology Progress Series 492: 21-39, 2013.

776 Lionard, M., Muylaert, K., Hanoutti, A., Maris, T., Tackx, M. and Vyverman W. Inter-annual
777 variability in phytoplankton summer blooms in the freshwater tidal reaches of the
778 Schelde estuary (Belgium). Estuarine, Coastal and Shelf Science 79: 694-700, 2008.

779 Low-Decarie, E., Bell, G. and Fussman, G.F. CO_2 alters community composition and response
780 to nutrient enrichment of freshwater phytoplankton. Oecologia 177: 875-883, 2015.

781 Meybeck, M. Global analyses of river systems: from Earth system controls to Anthropocene
782 syndromes. Phil. Trans. R. Soc. Lond. B 358: 1935-1955, 2003.

783 Middelburg, J. J., and Herman, P.M.J. Organic matter processing in tidal estuaries. Marine
784 Chemistry 106: 127-147, 2007.

785 Moran, M. A., W. M. Sheldon, and J. E. Sheldon. Biodegradation of riverine dissolved organic
786 carbon in five estuaries of the southeastern United States. Estuaries 22: 55-64, 1999.

787 Morton, R. and Henderson, B.L. Estimation of non-linear trends in water quality: an improved
788 approach using generalized additive models. Water Resources Research 44: W07420,
789 2008.

790 Murphy, R. R., Perry, E., Harcum, J. and Keisman, J. A Generalized Additive Model approach
791 to evaluating water quality: Chesapeake Bay case study. Environmental Modelling and
792 Software 118: 1-13, 2019.

793 Muylaert, K., Tackx, M. and Vyverman, W. Phytoplankton growth rates in the tidal freshwater
794 reaches of the Schelde estuary (Belgium) estimated using a simple light-limited primary
795 production model. Hydrobiologia 540: 127-140, 2005.

796 Noe, G. B. and Hupp, C.R. Retention of riverine sediment and nutrient loads by Coastal Plain
797 floodplains. Ecosystems 12: 728-746, 2009.

798 Orth, D.J., Jiao, Y., Schmidt, J.D., Hilling, C.D., Emmel J.A. and Fabrizio, M.C. Dynamics and
799 Role of Non-native Blue Catfish *Ictalurus furcatus* in Virginia's Tidal Waters. Final
800 Report submitted to Virginia Department of Game and Inland Fisheries. DOI:
801 10.13140/RG.2.2.35917.54246, 2017.

802 Patrick, C. J. and others. A system level analysis of coastal ecosystem responses to hurricane
803 impacts. Estuaries and Coasts 43: 943-959, 2020.

804 Qin, Q. and Shen, J. The contribution of local and transport processes to phytoplankton biomass
805 variability over different time scales in the Upper James River, Virginia. Estuarine,
806 Coastal and Shelf Science 196: 123-133, 2017.

807 Raymond, P. A., Bauer, J.E. and Cole, J.J. Atmospheric CO_2 evasion, dissolved inorganic
808 carbon production, and net heterotrophy in the York River estuary. Limnology and
809 Oceanography 45: 1707-1717, 2000.

810 Raymond, P. A., Caraco, N.F. and Cole, J.J. Carbon dioxide concentration and atmospheric flux
811 in the Hudson River. Estuaries 20: 381-390, 1997.

812 Raymond, P. A. and Cole, J.J. Gas exchange in rivers and estuaries: Choosing a gas transfer
813 velocity. Estuaries 24: 312-317, 2001.

814 Raymond, P. A., Hartmann, J., Lauerwald, R., Sobek, S., McDonald, C.P., Hoover, M., Butman,
815 D., Striegl, R.G., Mayorga, E., Humborg, C., Kortelainen, P., Durr, H., Meybeck, M.,
816 Ciais, P. and Guth, P. Global carbon dioxide emissions from inland waters. Nature 503:
817 355-359, 2017.

818 Raymond, P. A., and J. E. Bauer. Bacterial consumption of DOC during transport through a
819 temperate estuary. Aquatic Microbial Ecology 22: 1-12, 2000.

820 Raymond, P. A., and C. S. Hopkinson. Ecosystem modulation of dissolved carbon age in a
821 temperate marsh-dominated estuary. Ecosystems 6: 694-705, 2003.

822 Reiman, J. H. and Xu, Y.J. Diel variability of PCO_2 and CO_2 outgassing from the lower
823 Mississippi River: implications for riverine CO_2 outgassing estimation. Water 11: 43,
824 2019.

825 Richey, J. E., Melack, J.M., Aufdenkampe, A., Ballester, V.M. and Hess, L.L. Outgassing from
826 Amazonian rivers and wetlands as a large tropical source of atmospheric CO_2. Nature
827 416: 617-620, 2002.

828 Robson, B. J., Bukaveckas, P.A. and Hamilton, D.P. Modelling and mass balance assessments
829 of nutrient retention in a seasonally-flowing estuary (Swan River Estuary, Western
830 Australia). Estuarine, Coastal and Shelf Science 76: 282-292, 2008.

831 Ruegg, J., Conn, C.C., Anderson, E.P., Battin, T.J., Bernhardt, E.S., Canadell, M.B., Bonjour,
832 S.M., Hosen, J.D., Marzolf, N.S. and Yackulic, C.B. Thinking like a consumer: linking
833 aquatic basal metabolism and consumer dynamics. Limnology and Oceanography:
834 Letters 6: 1-17, 2021.

835 Schmitt, J. D., Peoples, B.K., Castello, L. and Orth, D.J. Feeding ecology of generalist
836 consumers: a case study of invasive blue catfish Ictalurus furcatus in Chesapeake Bay,
837 Virginia, USA. Environmental Biology of Fishes 102: 443-465, 2019.

838 Smock, L. A., A. B. Wright, and A. C. Benke 2005. Atlantic coast rivers of the southeastern
839 United States, p. 73-122. *In* [eds.], A. C. Benke and C. E. Cushing Rivers of North
840 America. Elsevier Academic Press.

841 Stedmon, C. A., S. Markager, M. Sondergaard, T. Vang, A. Laubel, N. H. Borch, and A.
842 Windelin. Dissolved organic matter (DOM) export to a temperate estuary: Seasonal
843 variations and implications of land use. Estuaries and Coasts 29: 388-400, 2006.

844 Steen, A.D., Quigley L.M. and Buchan, A. Evidence for the priming effect in a planktonic
845 estuarine microbial community. Frontiers in Marine Science 3:6.
846 doi:10.3389/fmars.2016.00006, 2015.

847 Tassone, S. and Bukaveckas, P.A. Seasonal, interannual and longitudinal patterns in estuarine
848 metabolism derived from diel oxygen data using multiple computational approaches.
849 Estuaries and Coasts 42: 1032-1051, 2019.

850 Thorp, J. H. and Bowes, R.E. Carbon sources in riverine food webs: new evidence from amino
851 acid isotope techniques. Ecosystems 20: 1029-1041, 2017.

852 Tranvik, L. J., Downing, J.A., Cotner, J.B. and others. Lakes and reservoirs as regulators of
853 carbon cycling and climate. Limnology and Oceanography 54: 2298-2314, 2009.

854 Tranvik, L. J., Cole, J.J. and Prairie, Y.T. The study of carbon in inland waters - from isolated
855 ecosystems to players in the global carbon cycle. Limnology and Oceanography: Letters
856 3: 41-48, 2018.

857 Tzortziou, M., P. J. Neale, C. L. Osburn, J. P. Megonigal, N. Maie, and R. Jaffe. Tidal marshes
858 as a source of optically and chemically distinctive colored dissolved organic matter in the
859 Chesapeake Bay. Limnology and Oceanography 53: 148-159, 2008.

860 Van Dam, B. R., Crosswell, J.R. and Paerl, H.W. Flood-driven CO_2 emissions from adjacent
861 North Carolina estuaries during Hurricane Joaquin (2015). Marine Chemistry 207: 1-12,
862 2018.

863 Vincent, W. F., Dodson, J.J., Bertrand, N. and Frenette, J-J. Photosynthetic and bacterial
864 production gradients in a larval fish nursery: The St. Lawrence River transition zone.
865 Marine Ecology Progress Series 139: 227-238, 1996.

866 Volta, C., Laruelle, G.G. and Regnier, P. Regional carbon and CO_2 budgets of North Sea tidal
867 estuaries. Estuarine, Coastal and Shelf Science 176: 76-90, 2016.

868 Vorosmarty, C. J., Meybeck, M., Fekete, B.M., Sharma, K.P., Green, P. and Syvitski, J.P.M.
869 Anthropogenic sediment retention: major global impact from registered river
870 impoundments. Global and Planetary Change 39: 169-190, 2013.

871 Voss, M., and others. Origin and fate of dissolved organic matter in four shallow Baltic Sea
872 estuaries. Biogeochemistry doi.org/10.1007/s10533-020-00703-5, 2020.

873 Ward, N. D. and others. The reactivity of plant-derived organic matter and the potential
874 importance of priming effects in the lower Amazon River. JGR-Biogeosciences 121:
875 1522–1539, 2016.

876 Ward, N. D., Bianchi, T.S., Medeiros, P.M., Seidel, M., Richey, J.E., Keil, R.G. and Sawakuchi,
877 H.O. Where carbon goes when water flows: carbon cycling across the aquatic
878 continuum. Frontiers in Marine Science 4: 7, 2017.

879 Wiegner, T. N., S. P. Seitzinger, P. M. Gilbert, and D. A. Bronk. Bioavailability of dissolved
880 organic nitrogen and carbon from nine rivers in the eastern United States. Aquatic
881 Microbial Ecology 43: 277-287, 2006.

882 Wiik, E., Haig, H.A., Hayes, N.M., Finlay, K., Simpson, G.L., Vogt, R.J. and Leavitt, P.R.
883 Generalized additive models of climatic and metabolic controls of subannual variation in
884 pCO_2 in productive hardwater lakes. Journal of Geophysical Research: Biogeosciences
885 123: 1940-1959, 2021.

886 Wood, J. D. and Bukaveckas, P.A. Increasing severity of phytoplankton nutrient limitation
887 following reductions in point source inputs to the tidal freshwater segment of the James
888 River Estuary. Estuaries and Coasts 37: 1188-1201, 2014.

889 Wood, J. D., Elliott, D., Garman, G.C., Hopler, D., Lee, W.M., McIninch, S., Porter, A.J. and
890 Bukaveckas, P.A. Autochthony, allochthony and the role of consumers in influencing the
891 sensitivity of aquatic systems to nutrient enrichment. Food Webs 7: 1-12, 2016.

892 Wood, S. Generalized Additive Models: an Introduction with R, 1 ed. Chapman and Hall/CRC,
893 Boca Raton, FL, 2006.

894 Wymore, A. S., Fazekas, H.M. and McDowell, W.H. Quantifying the frequency of synchronous
895 carbon and nitrogen export to the river network. Biogeochemistry 152: 1-12, 2021.

896 Xu, X. and others. Tidal freshwater zones as hotspots for biogeochemical cycling: sediment
897 organic matter decomposition in the lower reaches of two South Texas rivers. Estuaries
898 and Coasts 44 : 722-733, 2021.

899 Yang, G. and Moyer, D.L. Estimation of non-linear water quality trends in high-frequency
900 monitoring data. Science of the Total Environment 715: 136686, 2020.

901 Young, M., Hoew, E., O'Rear, T., Berridge, K. and Moyle, P. Food web fuel differs across
902 habitats and seasons of a tidal freshwater estuary. Estuaries and Coasts 44: 286-301,
903 2021.

904 Zarnetske, J. P., Bouda, M., Abbott, B.W., Saiers, J. and Raymond, P.A. Generality of
905 hydrologic transport limitation of watershed organic carbon flux across ecoregions of the
906 United States. Geophysical Research Letters 45: 11702-11711, 2018.

907

908 Table 1. Data collection sites for this study include USGS Fall Line gauging stations (Q denotes
909 discharge), estuarine sampling sites and an ungauged Coastal Plain tributary of the James
910 (Kimages Creek). Station numbers denote distance in river miles from the confluence with
911 Chesapeake Bay (James) or the York (Pamunkey and Mattaponi). Observations denote the
912 number of sampling dates for water chemistry within the specified time span.

Tributary	Segment	Stations	Parameters	Years	Observations	Source
James	River	JMS110	Q, DOC, POC	2010-19	197	USGS (02037500)
		JMS110	Cl, DIC, pCO_2	2012-19	189	This Study
	Estuary	JMS99,75,69,56	Cl, DOC, POC, DIC, pCO_2	2015-19	105	This Study
	Ungauged	Kimages Creek	Cl, DOC, POC, DIC, pCO2	2012-19	211	This Study
Pamunkey	River	PMK82	Q, DOC, POC	2010-19	202	USGS (01673000)
	Estuary	PMK50,39,6	DOC, POC, DIC, pCO_2	2017-19	60	This Study
Mattaponi	River	MPN54	Q, DOC, POC	2010-19	203	USGS (01674500)
	Estuary	MPN36,29,4	DOC, POC, DIC, pCO_2	2017-19	60	This Study

913

914

915 Table 2. GAM analysis of seasonal (day of year; DOY), inter-annual (date) and discharge
916 dependent variation in river, tributary and estuarine DOC, POC, DIC, pCO_2 and Cl. Data are for
917 riverine and upper estuarine segments of the James, Mattaponi and Pamunkey as well as a local
918 (below Fall Line) tributary (Kimages Creek). Statistics include the adjusted R^2, root mean
919 square error (RMSE as mg L^{-1}, except pCO_2 = ppmv), and significance of s values with their
920 effective degrees of freedom (** denotes $p < 0.001$; * $p < 0.05$).

921

Model	Fraction	Site	Adj R^2	RMSE	s(DOY)	s(date)	s(discharge)
River	DOC	James	0.50	0.82	3.42**	8.52**	3.00**
		Mattaponi	0.81	1.00	5.66**	8.93**	5.43**
		Pamunkey	0.67	1.06	4.64**	8.61**	5.54**
	POC	James	0.76	1.74	3.67**	7.89**	8.20**
		Mattaponi	0.38	0.61	3.99**	6.34	6.25**
		Pamunkey	0.51	1.08	2.39**	8.95**	7.79**
	DIC	James	0.44	4.19	2.42**	7.89**	8.20**
	pCO_2	James	0.67	149	3.37**	6.43**	3.59**
	Cl	James	0.48	4.36	7.23**	8.30**	6.73**
Tributary	DOC	Kimages	0.33	3.22	4.70**	8.26**	NA
	POC	Kimages	0.24	0.57	4.61**	7.63**	NA
	DIC	Kimages	0.19	3.00	0.41	8.26**	NA
	Cl	Kimages	0.23	8.63	6.46**	6.48**	NA
Estuary	DOC	James	0.13	3.44	4.29	1.96	1.91*
		Mattaponi	0.27	2.37	5.65	3.42**	1.00
		Pamunkey	0.27	2.61	5.94*	3.95**	1.00
	POC	James	0.75	0.22	5.77**	2.64**	3.68**
		Mattaponi	0.14	0.53	1.79*	1.00	4.13**
		Pamunkey	0.40	0.30	2.46**	1.27	7.59**
	DIC	James	0.76	1.55	1.27**	4.41**	2.50**
		Mattaponi	0.74	2.05	1.74**	2.27**	1.48**
		Pamunkey	0.68	2.10	1.30*	3.16**	1.00**
	pCO_2	James	0.40	241	5.84**	3.48	2.38*
		Mattaponi	0.82	367	3.31**	2.65**	4.14**
		Pamunkey	0.81	357	3.81**	2.73**	4.01**
	Cl	James	0.46	24.7	6.26**	8.54**	6.97**

922

923

Figure 1. Map showing USGS discharge gauging locations, estuarine sampling sites and continuous dissolved oxygen monitoring locations on the Mattaponi, Pamunkey and James. Inset: James and York watersheds in relation to physiographic provinces.

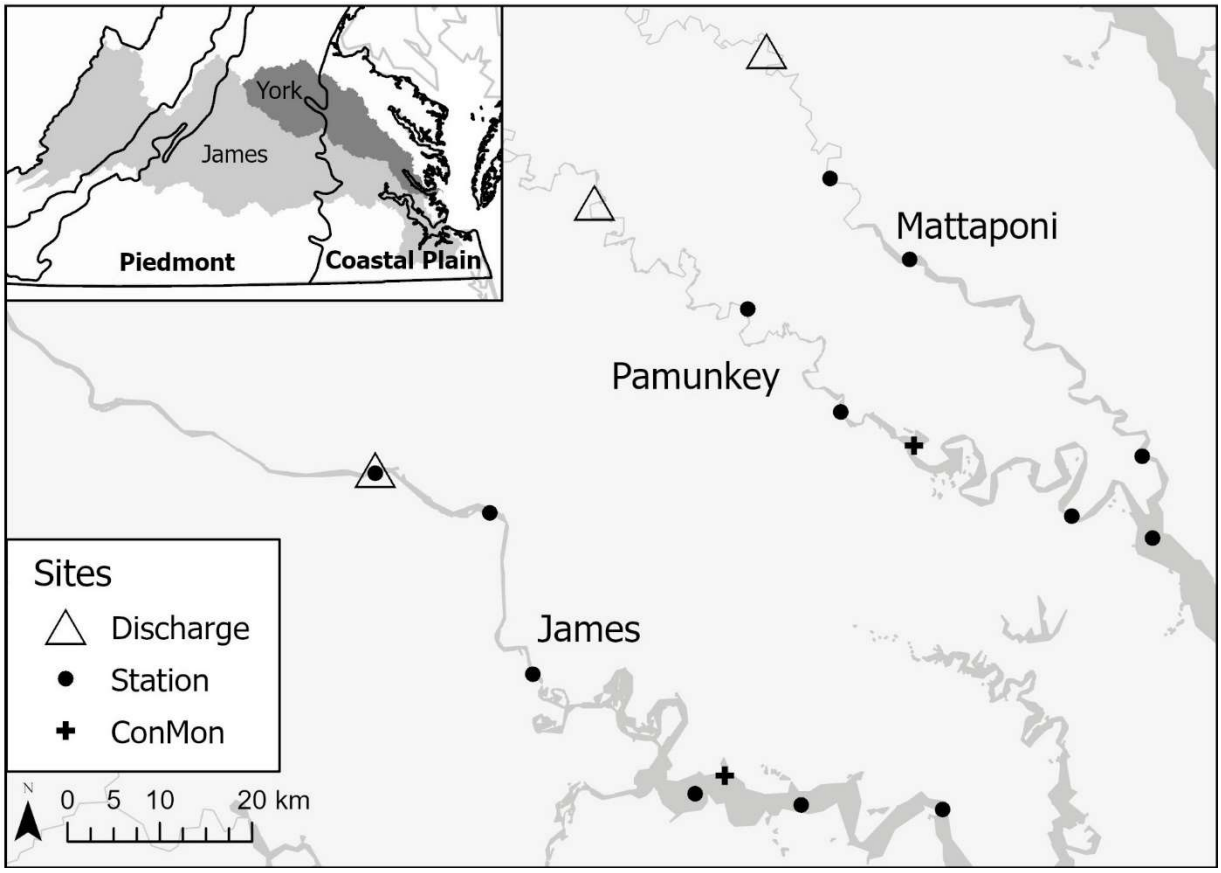

Figure 2. Seasonal variation in instantaneous discharge measured at the Fall Line of the James, Mattaponi and Pamunkey Rivers. Here and in subsequent figures, symbols denote median (bar), 25 and 75 %-tiles (box), 5 and 95 %-tiles (whiskers) and outliers (dots).

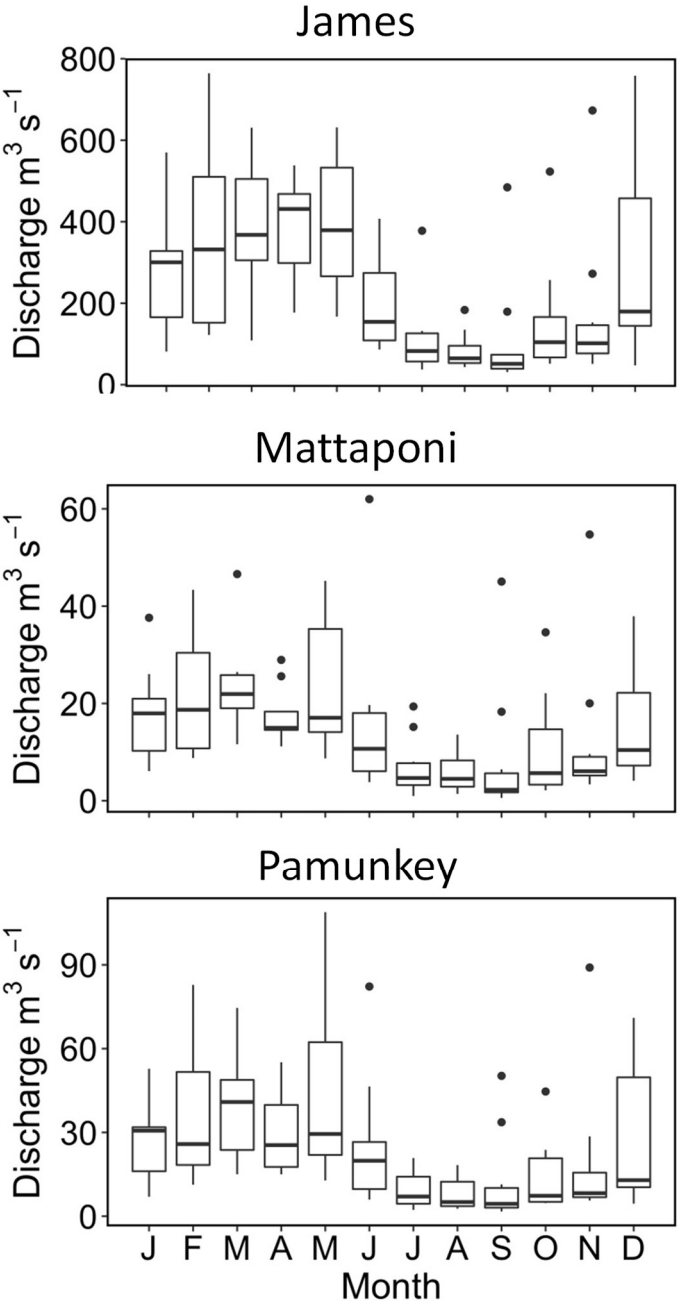

Figure 3. Time series of Cl concentrations in the tidal fresh segment of the James Estuary (upper panel) and Cl fluxes associated with river inputs, estuarine export and net tidal exchange (lower panels).

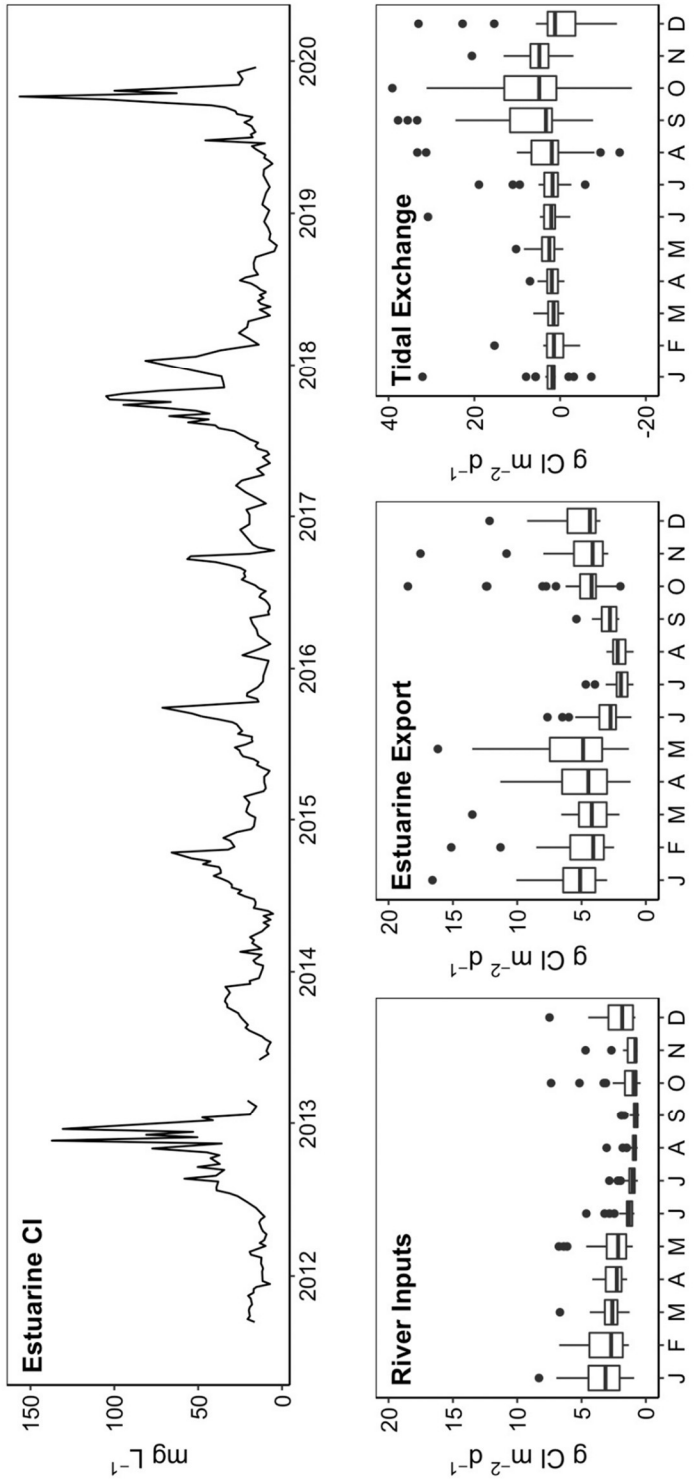

Figure 4. Results from GAM analysis depicting changes in riverine DOC, POC and DIC as a function of discharge (Q) for the James Mattaponi and Pamunkey Rivers.

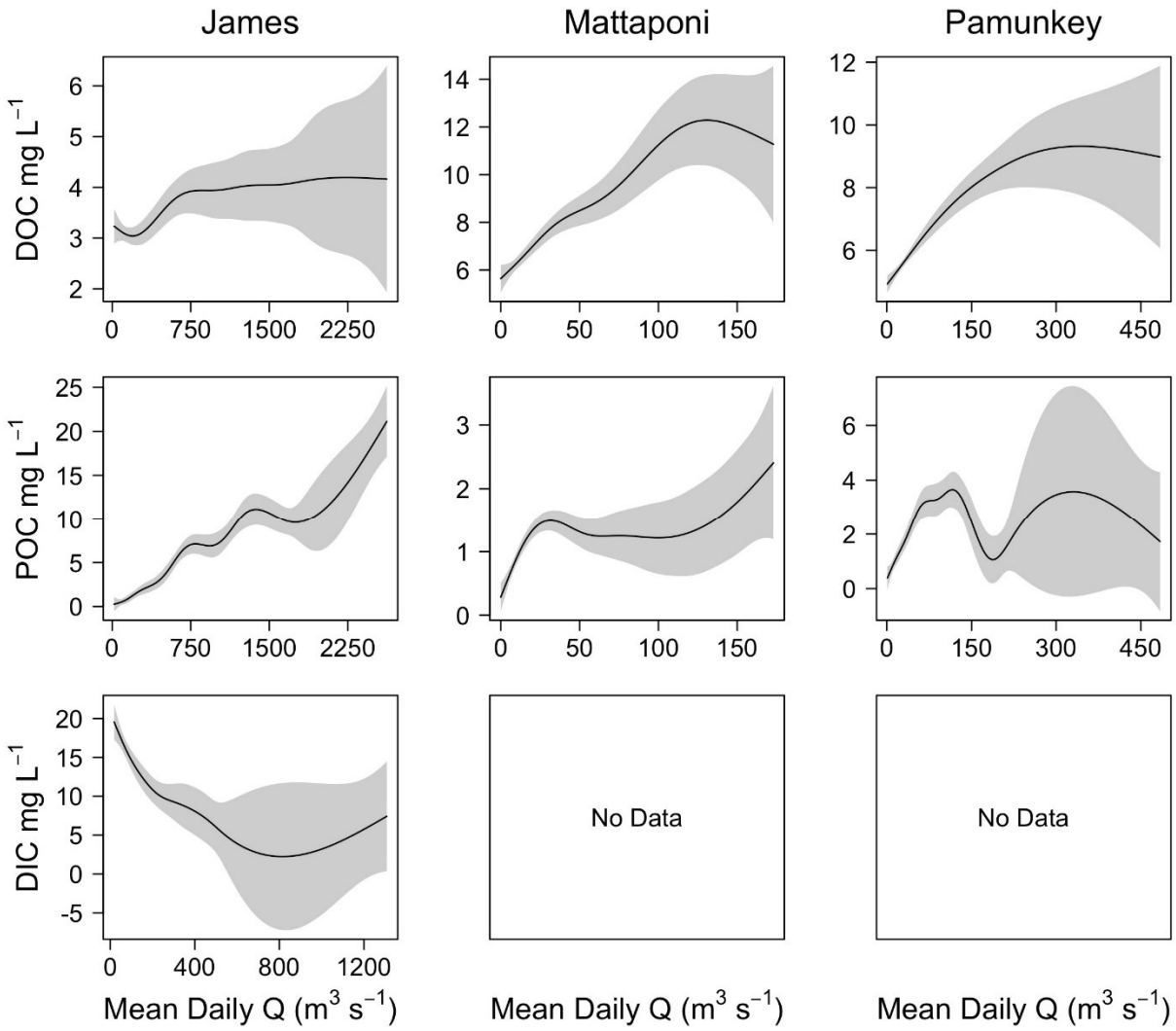

Figure 5. Results from GAM analysis depicting the effects of discharge (Q) on estuarine DOC, POC and DIC for the James Mattaponi and Pamunkey Estuaries. Concentrations are volume-weighted averages among estuarine sampling locations.

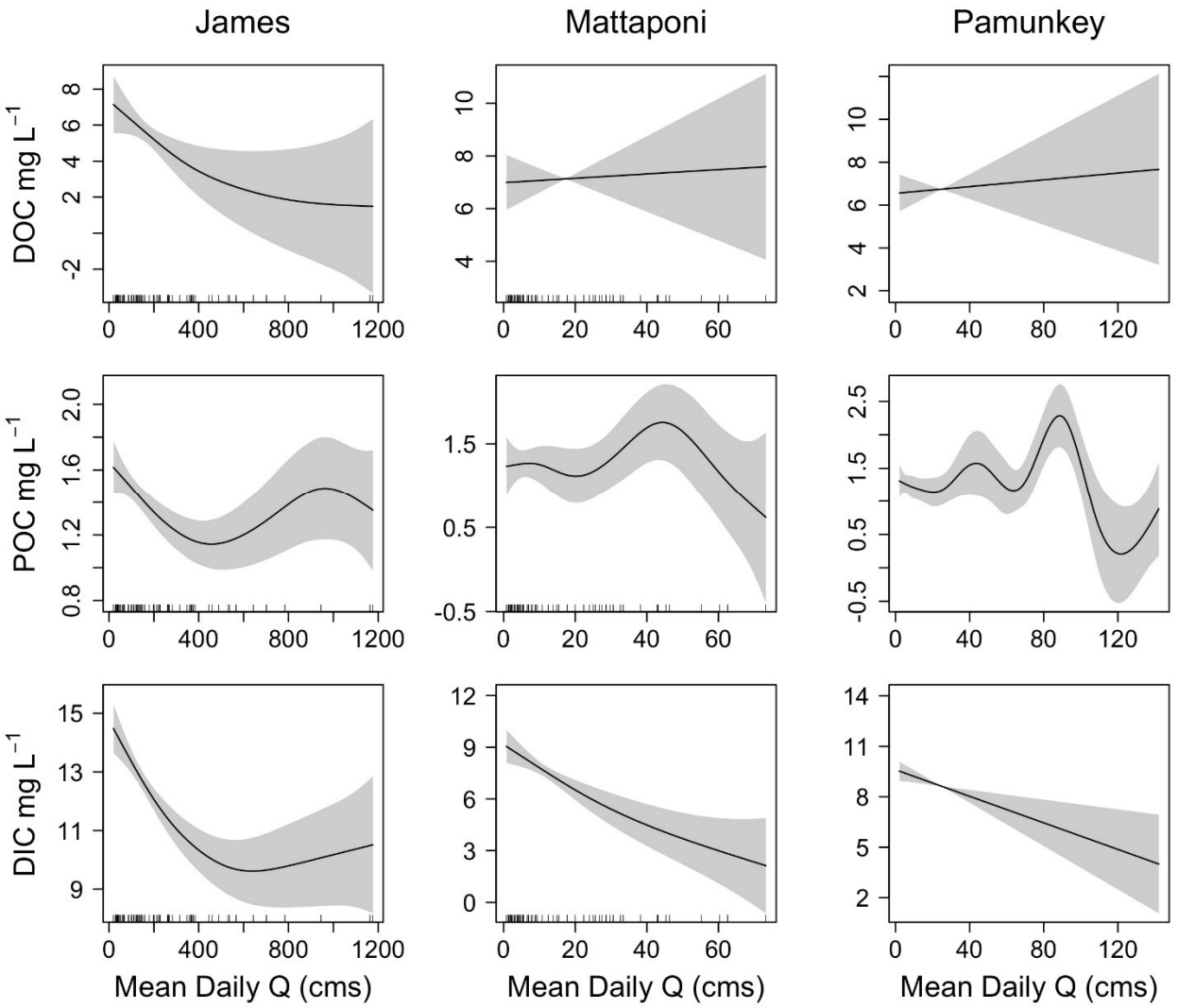

Figure 6. Results from GAM analysis depicting seasonal (day of year; DOY), inter-annual (decimal date) and discharge dependent variation in pCO_2 of the James, Mattaponi and Pamunkey Estuaries. Analyses were based on volume-weighted averages from 3-4 sampling locations in each estuary.

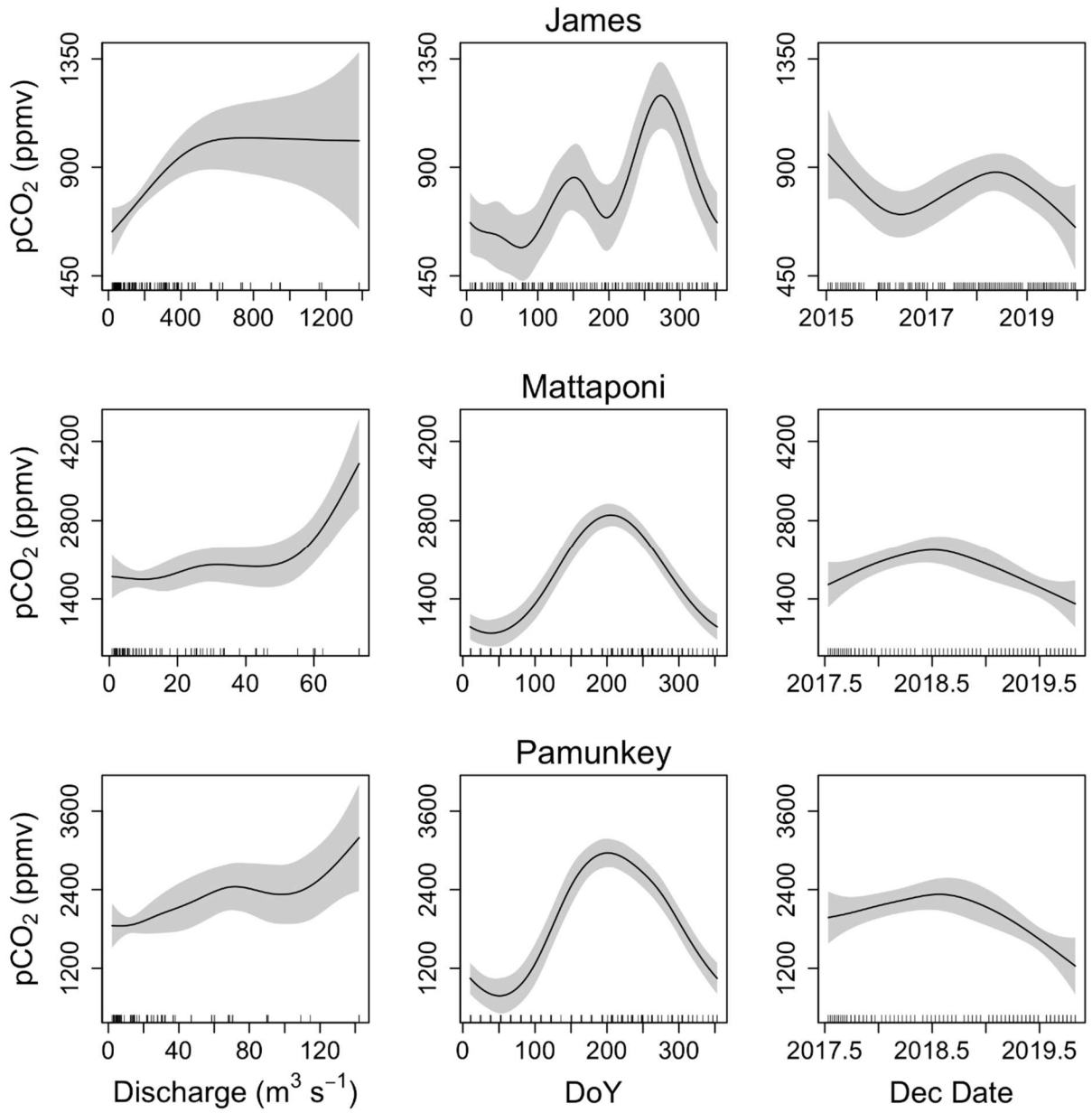

Figure 7. Monthly average values of air-water CO_2 fluxes for the James, Mattaponi and Pamunkey Estuaries. Positive values denote efflux of CO_2 from the estuary.

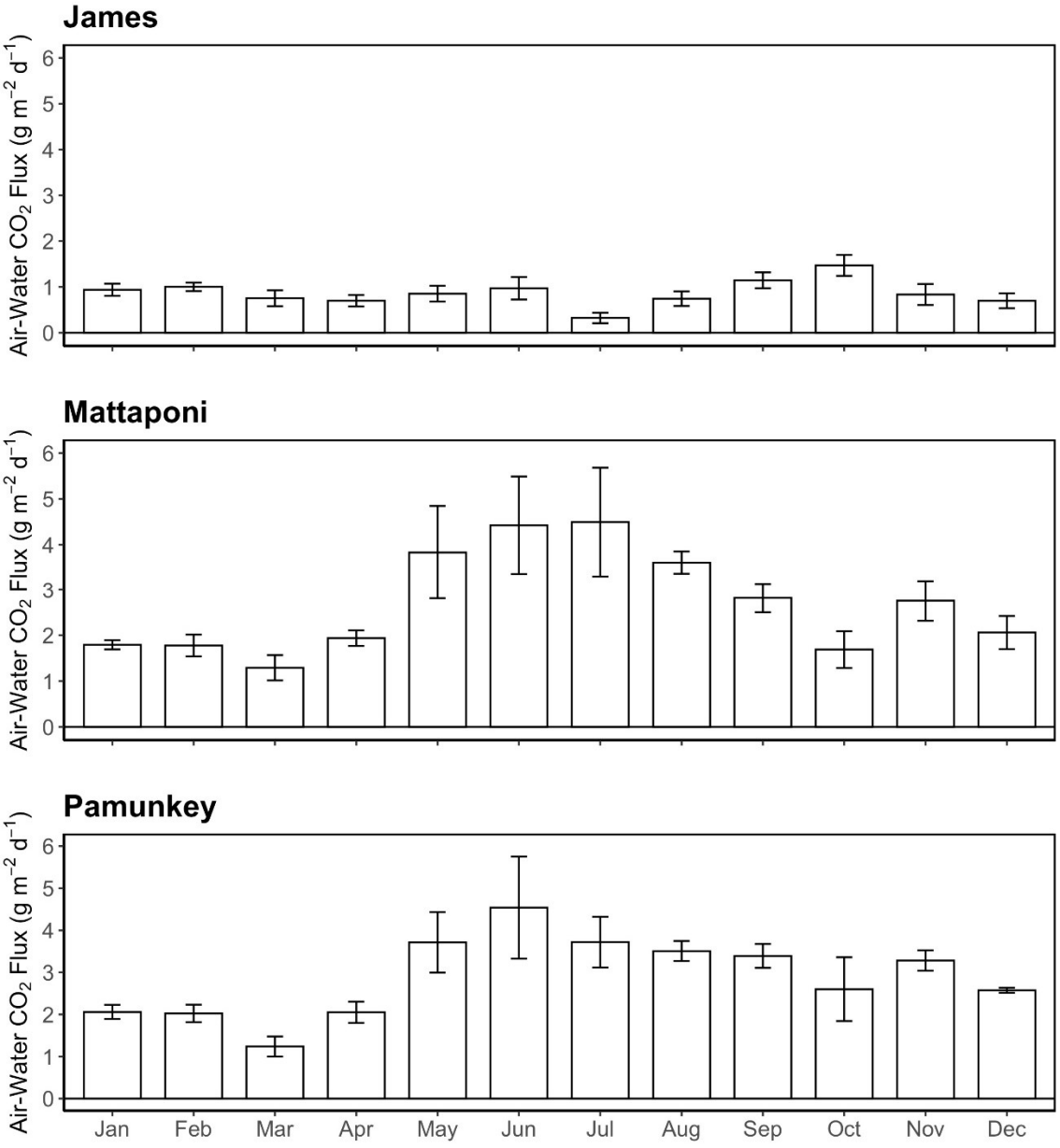

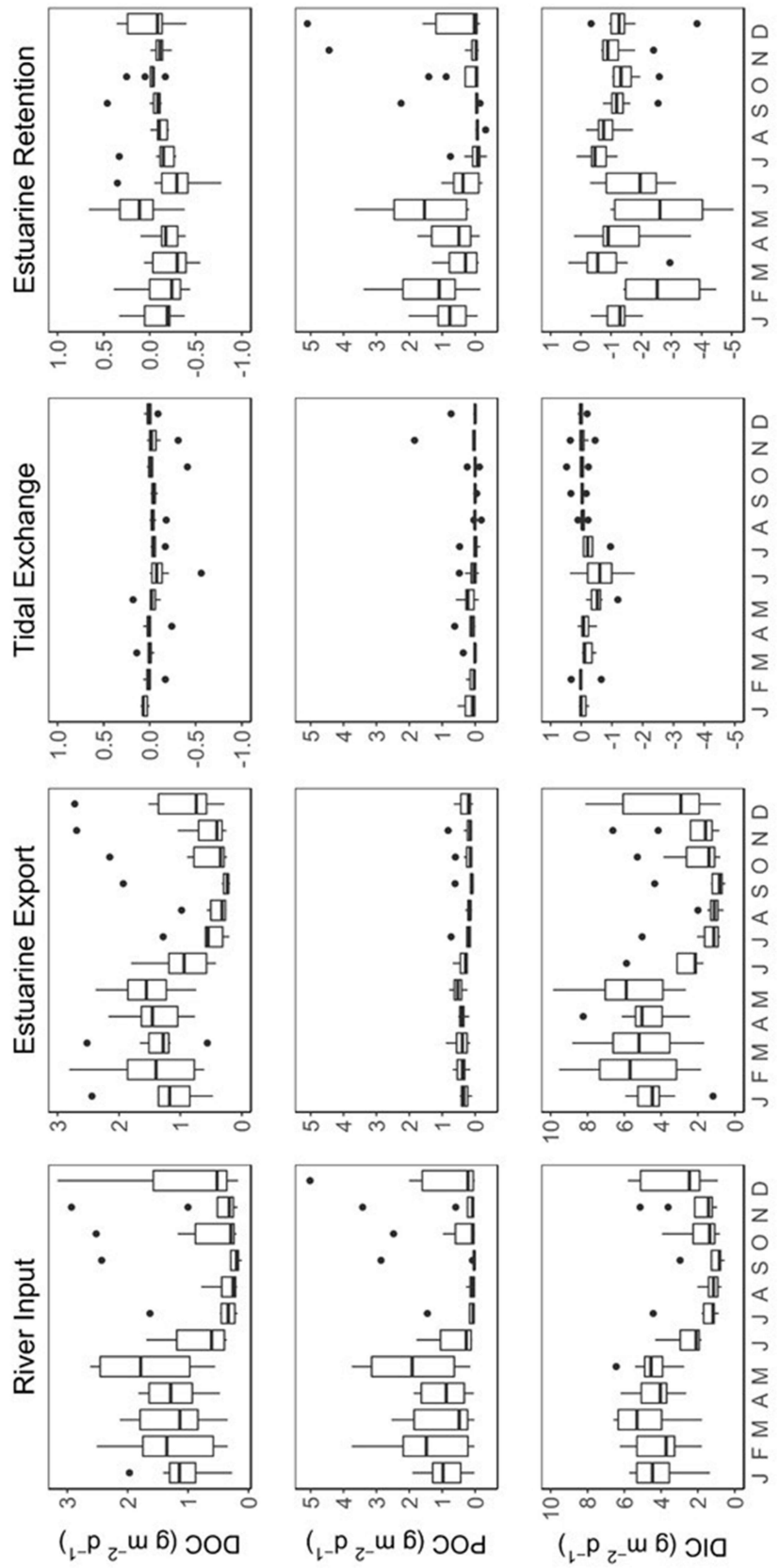

Figure 8. Seasonal variation in DOC, POC and DIC fluxes associated with riverine inputs, estuarine export, tidal exchange and estuarine retention for the tidal freshwater segment of the James Estuary (note differences in y axis scaling). Negative values for estuarine retention denote a net loss. DIC retention estimates take into account atmospheric losses of CO_2.

Figure 9. River input and estuarine export fluxes of DOC and POC for the Pamunkey (PMK) and Mattaponi (MPN) estuaries.

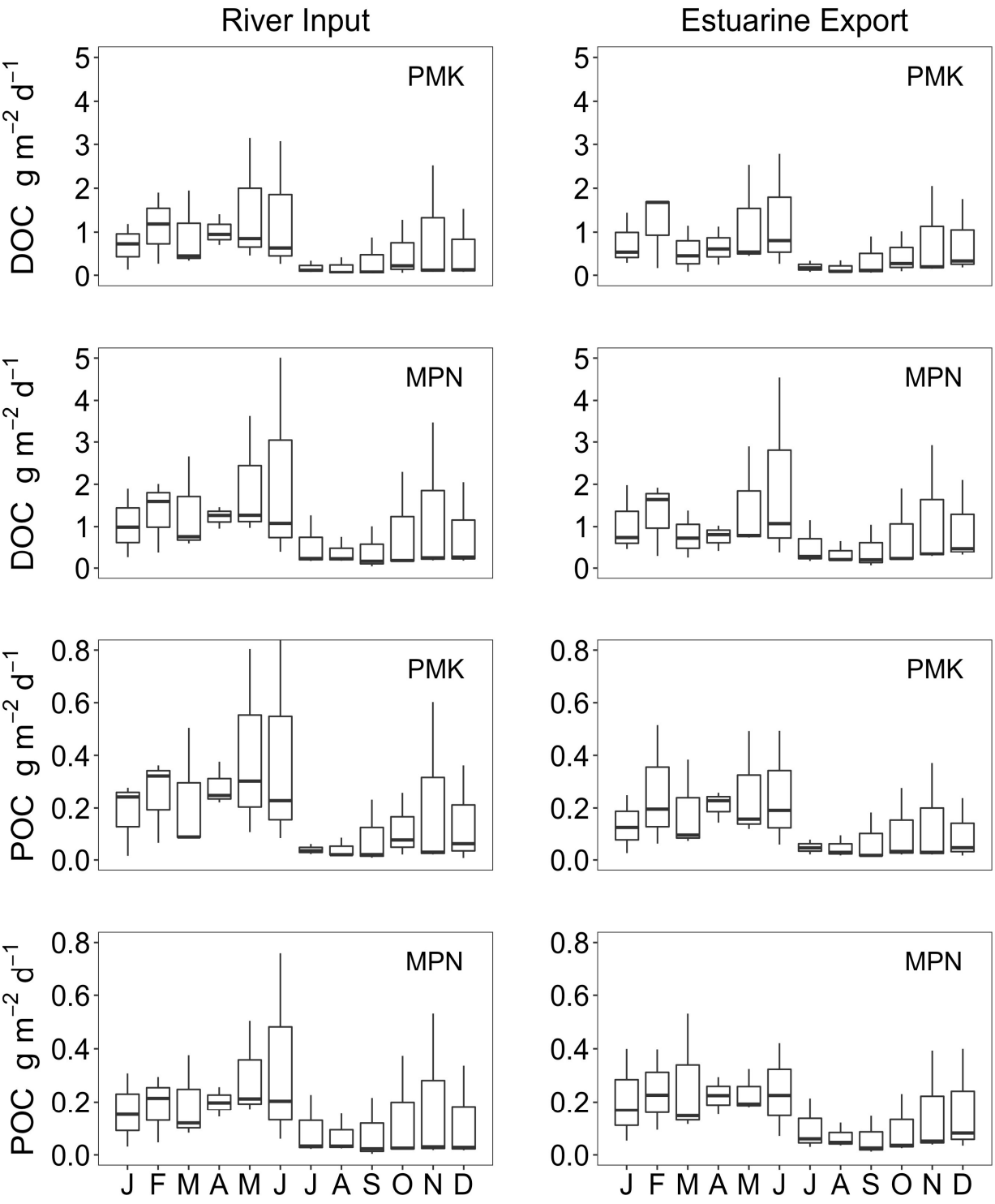

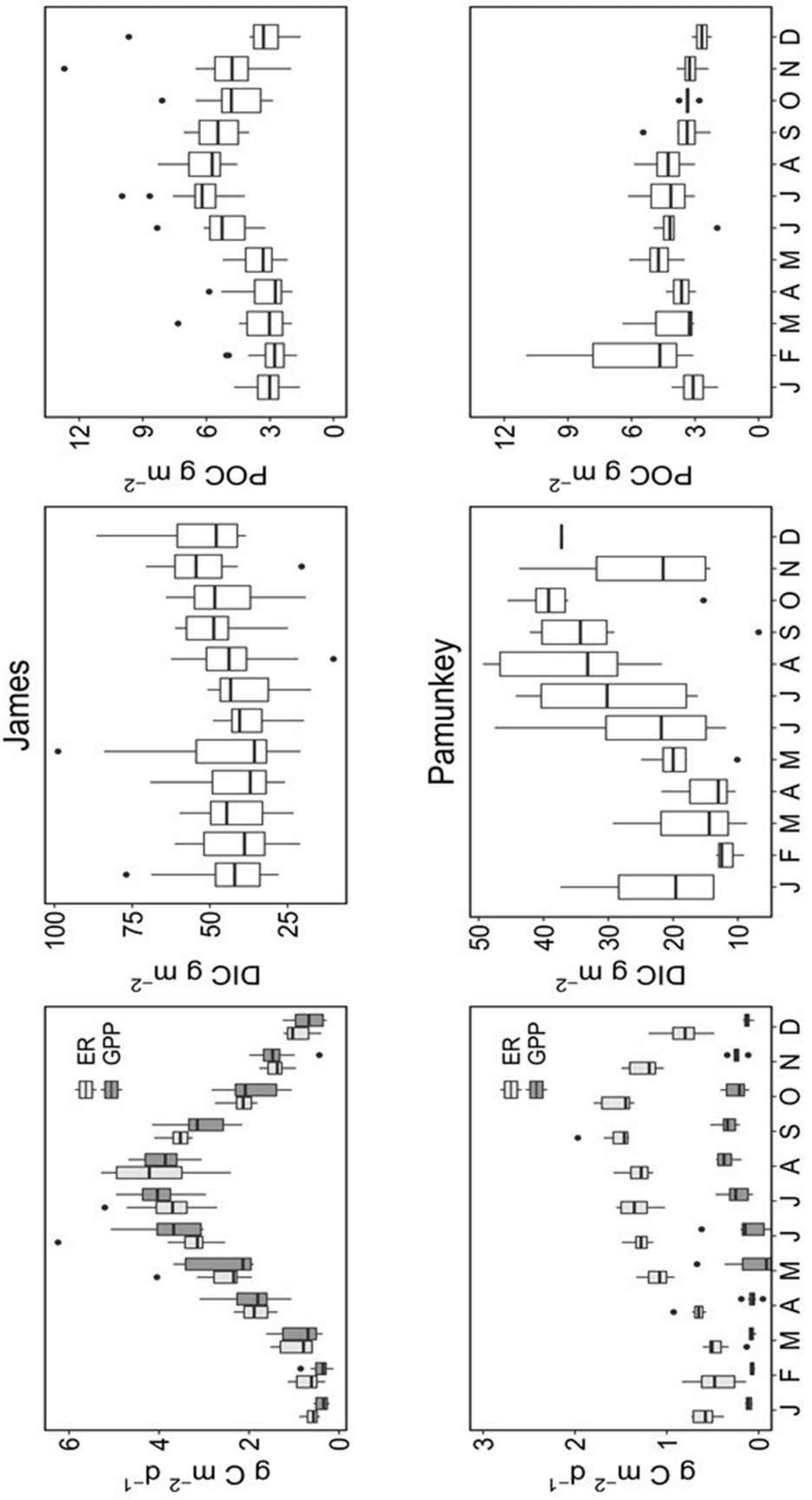

Figure 10. Seasonal variation in ecosystem metabolism (GPP and ER) in comparison to DIC and POC concentrations in the James and Pamunkey estuaries.

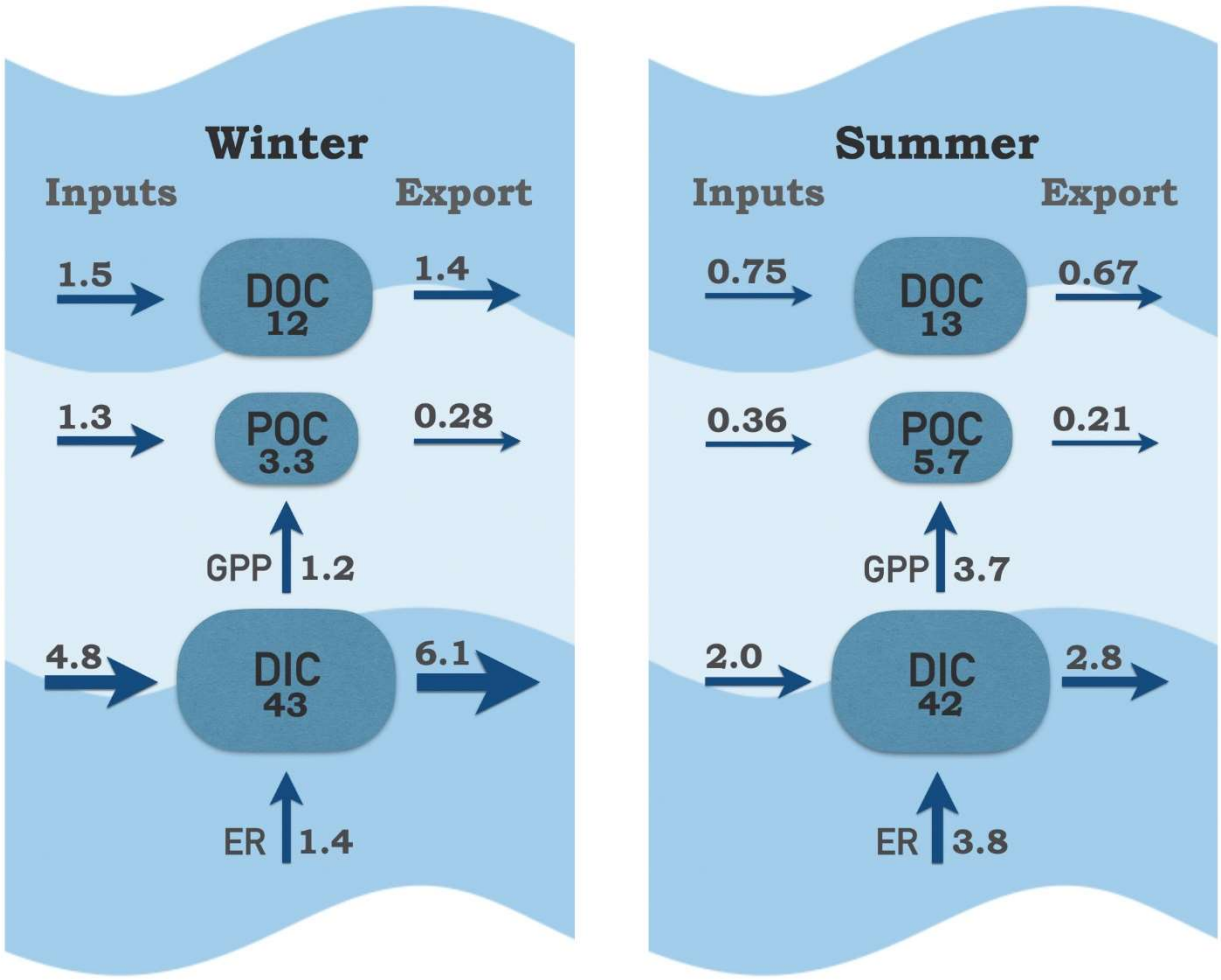

Figure 11. Carbon pools and fluxes within the tidal fresh segment of the James Estuary during winter (Jan-May) and summer (June-Sept). Inputs include riverine, local tributary and point source contributions; exports include tidal exchange and atmospheric losses of CO_2. Carbon pools (boxes) are g C m^{-2}; fluxes (arrows) are g C m^{-2} d^{-1}.